MACROPHAGE IRON CONTENT AND EXACERBATIONS OF COPD

EXAMINING THE ROLE OF EXCESS AIRWAY MACROPHAGE IRON ON INFECTIVE
COPD EXACERBATIONS AND POTENTIAL MECHANISMS

By TERENCE HO, M.B., B.Ch., B.A.O., M.Sc.(OT), B.Kin

A thesis submitted to the School of Graduate Studies in Partial Fulfilment of the
Requirements for the Degree Master of Science

Descriptive Note

McMaster University MASTER OF SCIENCE (2019) Hamilton, Ontario (Medical Sciences)

TITLE: Examining the role of excess airway macrophage iron on infective COPD exacerbations and potential mechanisms AUTHOR: Terence Ho, M.B., B.Ch., B.A.O. (University College Cork), M.Sc.(OT-McMaster University), B.Kin (McMaster University) SUPERVISOR: Professor P.K. Nair NUMBER OF PAGES: 124

Lay Abstract

COPD patients often require hospitalization due to respiratory infections (bacterial or viral) that result in worsening of their breathing. It is difficult to predict who is at high risk for this to occur, which makes it harder to prevent. Many species of bacteria depend on iron as a nutrient. We wanted to see if iron being present in certain immune cells (macrophages) in the sputum could predict these flares by: testing how iron enters these cells, seeing if bacterial growth is altered by putting iron into these cells, and following a group of COPD patients and seeing if those with higher iron in their sputum had higher risk of infectious flares. Though more testing is needed, we found that a protein often present with chronic inflammation may be associated with higher sputum macrophage iron, and that there is evidence that killing of bacteria in COPD sputum macrophages is lower with high iron, and that patients with higher sputum iron are at greater risk of having infectious flares.

Abstract

Background: Many COPD patients have recurrent exacerbations due to infection, but there are no valid predictors of this phenotype. Previously an observational study showed that higher iron content in sputum macrophages was associated with infectious exacerbations.

Objectives: The thesis aimed to assess the mechanisms of pulmonary macrophage iron sequestration, test the effect of macrophage iron-loading on bacterial uptake and killing, and prospectively determine if sputum hemosiderin index can predict infectious exacerbations of COPD.

Methods: Intracellular iron was measured directly and indirectly in cell-line-derived and isolated sputum macrophages after treatment with exogenous IL-6, hepcidin or heat-inactivated *H.influenzae*. Bacterial uptake and killing were compared in both types of macrophages, in the presence or absence of iron-loading. A prospective cohort of COPD patients had their sputum hemosiderin index measured at baseline and were monitored for 1-year for infectious exacerbations requiring admission to hospital.

Results: For pulmonary iron sequestration, IL-6 appears important, but the role of hepcidin is not clear. Iron-loading reduced the uptake of COPD-relevant organisms by almost one-third in cell-line-derived macrophage, and there was a near-significant linear relationship between sputum hemosiderin index and killing of *H.influenzae* (p=0.075). In terms of infective exacerbations, FEV_1 had predictive utility (β=-0.051,

p=0.017) while a positive trend for sputum hemosiderin index (β=0.035, p=0.051)

suggests that this biomarker has clinical promise.

Conclusion: Through in vitro experiments and cohort data, we have established a

framework suggesting that excess iron in pulmonary macrophage may contribute to

recurrent bacterial airway infection in COPD. IL-6 appears to contribute to sputum

macrophage iron sequestration, which subsequently may lead to immune cell

dysfunction and ultimately result in an increased frequency of infective exacerbation.

Acknowledgements

Deciding to pursue a MSc in Medical Sciences after completing my respirology training was not a simple decision. In my mind, I had a clear goal of being an academic physician, as it would put me in a position where I could make the greatest impact on the lives of patients and our understanding of airway disease. I had such positive experiences with research during my fellowship, that I felt it was a real possibility to have research be central in my career. However, as I saw colleagues securing jobs in the community and thriving in that setting, and saw what was necessary to succeed in research, at times, I had feelings of insecurity surface. Though completing my MSc thesis and airways fellowship offers no guarantee of how I will fare as an academic physician or in research, it was an important step in proving to myself that if I continue to work hard, I have what it takes to succeed. Building this belief in myself was part and parcel of completing my MSc thesis, and was only made possible by the contributions of many individuals.

Firstly, I want to thank my supervisor, Dr. Parameswaran Nair, for believing in my potential and driving nearly the entirety of my research experiences. I have learned so much from him over the last three years, and know that this will likely continue for many years. I also must thank all the members of Dr. Nair's laboratory for their support and collective expertise. My supervisory committee, Dr. Gerard Cox, Dr. Martin Stampfli, and Dr. Michael Surette, were also invaluable for their insightful perspectives and guidance while completing my MSc degree.

Table of Contents

List of Figures

List of Tables

List of Abbreviations and Symbols

ACE   angiotensin converting enzyme

AECOPD   acute exacerbation of COPD

ANOVA   analysis of variance

AM   alveolar macrophages

BALF   bronchoalveolar lavage fluid

BMP   bone morphogenetic protein

BMPR   bone morphogenetic protein receptor

cDNA   complementary deoxyribonucleic acid

CF   cystic fibrosis

CFU   colony-forming units

COPD   chronic obstructive pulmonary disease

DMT1   divalent metal transporter-1

DTT   dithiothreitol

ELISA   enzyme-linked immunosorbent assay

$FeSO_4$ ferrous sulphate

FEV_1 forced expiratory volume in one second

FPN   ferroportin

FVC   forced vital capacity

H&E   hematoxylin and eosin

HAMP   hepcidin anti-microbial peptide gene

HBSS	Hank's balanced salt solution
HI	*Haemophilus influenzae*
hi-HI	heat-inactivated *Haemophilus influenzae*
HR	hazard ratio
ICP-MS	inductively-coupled mass spectrometry
IL-6	interleukin-6
IQR	interquartile range
JAK	Janus kinase
LABA	long-acting beta agonist
LAMA	long-acting muscarinic antagonist
LPS	lipopolysaccharide
Mø	macrophage
MC	*Moraxella catarrhalis*
MCV	mean cell volume
mRNA	messenger ribonucleic acid
NPS	nasopharyngeal swab
NRAMP1	natural resistance-associated macrophage protein-1
NTHI	non-typeable *Haemophilus influenzae*
PBMC	peripheral blood mononuclear cells
PBS	phosophate-buffered saline
PCR	respiratory virus polymerase chain reaction

PKY	pack-years
PMA	phorbol 12-myristate-13-acetate
PRR	pattern recognition receptors
RFU	relative fluorescence units
ROS	reactive oxygen species
RT-qPCR	real-time quantitative polymerase chain reaction
SHI	sputum hemosiderin index
SLC40A1	solute carrier family 40 member 1
SM	sputum macrophage
SNP	single nucleotide polymorphism
SP	*Streptococcus pneumoniae*
STAT	signal transducer and activator of transcription
TDM	Tamm-Horsfall Protein-1-derived macrophages
Tf	transferrin
TfR1	transferrin receptor-1
THP-1	Tamm-Horsfall Protein-1
THY	Todd-Hewitt broth
TLR	toll-like receptors
TMPRSS6	transmembrane serine protease 6
TSB	tryptic soy broth

Declaration of Academic Achievement

I, Terence Ho declare this thesis to be my own work. This document has been written by myself alone. The research work associated with this thesis was completed by myself with help from Katherine Radford (research technologist, Firestone Institute for Respiratory Health, who assisted with cell-line work and ELISA), Matt Nichols (post-doctoral fellow of Dr. Joesph Macri, McMaster University, who assisted with mass spectrometry), and Matt Devalaraja (US collaborator who assisted with detection of TMPRSS6 genetic polymorphisms. This work was supported by the Ministry of Health through a funded position in the Clinician Investigator Program, an Ontario Graduate Scholarship, and educational and travel grants from the Firestone Institute for Respiratory Health.

Chapter 1: Introduction

Introduction

<u>COPD and Acute Exacerbations</u>

Chronic obstructive pulmonary disease (COPD) is a respiratory condition characterized by progressive, partially reversible airflow limitation and frequent exacerbations (1). Its prevalence is estimated at 4.5%, and it is currently the fourth leading cause of death in Canada (1). Acute exacerbations of COPD (AECOPD) are the most common reason for admission to hospital in Canada (2), and airway infections are the cause in 50-70% of cases (3,4). This contributes to significant financial burden, with global costs estimated at $2.1 trillion annually with expectations that this figure will increase more than two-fold by 2030 (5).

A single AECOPD event increases the likelihood of negative health outcomes, including mortality and reduced lung function (6,7). Despite multiple guideline-based management strategies, the rates of recurrent AECOPD (≥1 AECOPD within 8 weeks of discharge) are 30% (6). This may be related to an incomplete understanding of exacerbations, in terms of reliable predictors (other than prior exacerbation), mechanisms of pathology, and hence ideal management strategies. Although there are oral medications targeted towards preventing recurrent AECOPD, they exhibit inconsistent and modest efficacy (8,9). There are several potential reasons that predispose patients with COPD to infective exacerbations. These range from innate immune dysfunctions due to cigarette smoke exposure, ciliary dysfunction, and

immunoglobulin deficiencies (10), to altered local metabolic environments which could

be conducive to microbial growth or impair leukocyte function (11).

Biological Function of Iron

Iron is a ubiquitous element and an essential nutrient to nearly all organisms (12). It is

most well-known for its structural role in forming hemoglobin, but it also is involved in

multiple aspects of cell function, including DNA biosynthesis, cell-cycle progression and

protein function (13). Iron is also necessary for the Fenton reaction, which generates the

reactive oxygen species (ROS) crucial for cellular bactericidal capacity (14).

Furthermore, Iron-overloaded conditions can contribute to the release of previously

phagocytosed organisms by precipitating a specific form of cell-death termed

"ferroptosis" (15).

The importance of iron homeostasis has become more prominent with the literature

identifying associations between chronic iron overload and various conditions, including

atherosclerosis, metabolic syndrome, Alzheimer's disease and malignancy (14).

Excess Iron and Susceptibility to Infection

One potential unrecognized mechanism for recurrent infective AECOPD is related to

excess respiratory iron. As iron is a growth essential nutrient for microbes, increased

iron may create a favourable environment for growth and increased virulence. In

systemic iron overload conditions (e.g. β-thalassemia), there is increased susceptibility

to sepsis and bacteremia (16). In the respiratory system, inhalation of iron has been

associated with pneumonia, influenza, active pulmonary tuberculosis, and infectious

bronchitis (17-20). Ex vivo studies of both murine lung and human cell-line macrophages

suggest iron-loading is associated with phagocytic dysfunction and/or reduced bacterial

killing (11,13,21).

The Potential Role of Iron in COPD

Explanted specimens from COPD patients have increased respiratory iron content, which

correlate with airflow obstruction and emphysema severity (22). The importance of iron

in COPD is supported by proteomic analyses which have identified that iron metabolism

genes were the strongest biomarker for COPD (23). Genome-wide association studies

identified that iron-responsive element-binding protein 2 is a susceptibility gene for

COPD (24). Furthermore, deletion of this gene in a mouse model confers protection

against airway remodeling. In this same study, chelation of free iron prevented cigarette

smoke-induced emphysema in mice (25).

Iron may increase COPD susceptibility by bacterial colonisation of the airways, which is

considered to be central to the pathogenesis of this condition. Previous studies have

noted impaired innate immune function of COPD macrophages (26), but macrophage

iron content was not directly measured in these studies, so it remains a potential

contributing factor. The effect of iron on macrophages is directly supported by cell-line studies of experimental iron-loading demonstrating lysosomal dysfunction and reduced bactericidal capacity (21), and improvement in bactericidal activity with chelation in murine alveolar macrophages (11). These types of experiments have not been done with respiratory-specific pathogens in mind, or in human airway macrophages.

Mechanisms of Pulmonary Iron Accumulation

Alveolar macrophages have multiple functions, including roles in lung development, surfactant homeostasis, and microbial clearance (27). In addition, they are also important for local iron-scavenging, and house the majority of the total respiratory iron content (22,28). Respiratory iron can accumulate in these cells secondary to cigarette smoke, inhaled iron, and raised left ventricular end-diastolic pressure (29,30). In the case of congestive heart failure, red blood cells extravasated from the pulmonary circulation are phagocytosed and their hemoglobin broken down into elemental iron.

The systemic regulation of iron has been well-described, with hepatocyte-mediated hepcidin release acting as the primary regulator of iron. It causes the degradation of ferroportin, the only known mammalian iron exporter, subsequently reducing the amount of extracellular iron. Ferroportin is present on many cell types, including macrophages and enterocytes, and thus its downregulation causes cellular sequestration (best described in splenic macrophages) and reduced absorption, respectively. The

release of hepcidin can be modulated by multiple factors (including high iron content), but most interestingly, is strongly regulated by chronic inflammation (31). This is best described in the pathophysiology of anemia of chronic disease, where chronic inflammatory mediators stimulate the release of Interleukin-6 (IL-6), which subsequently causes the release of hepcidin from hepatocytes (Figure 1) or myeloid leukocytes (Figure 2). This process is initially protective and deprives invading microbes of iron and reduces the generation of reactive oxygen species, but with sustained inflammation leads to iron-overload of splenic, and potentially lung macrophages (22,32,33). As a disease associated with chronic systemic inflammation (34), the mechanism in COPD may be analogous to anemia of chronic disease, and this is supported by the expression of both hepcidin and ferroportin in alveolar macrophages (35).
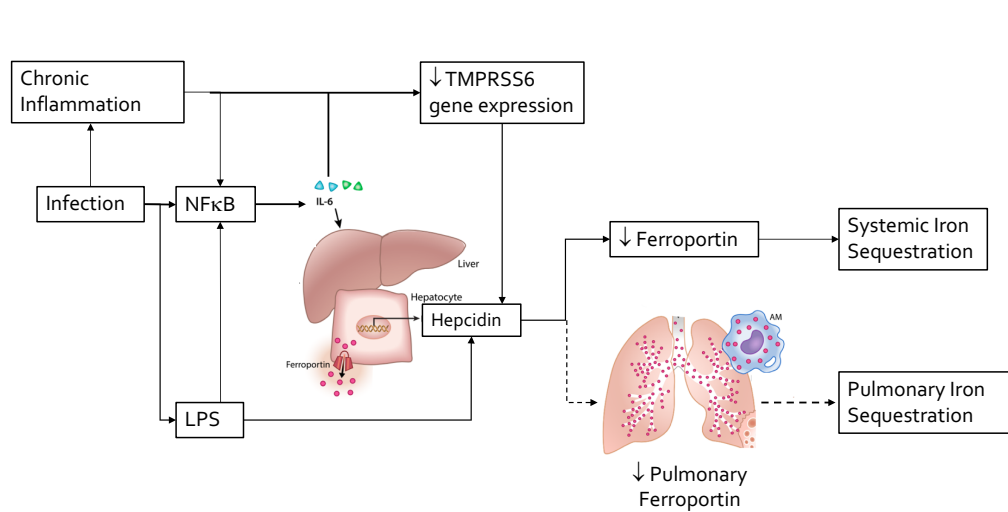
Figure 1: Interactions between infectious/inflammatory pathways and the hepatic component of the hepcidin-ferroportin axis. Dotted lines denote proposed mechanisms. Figure adapted from Cloonan et al. (2017). NFκB, nuclear factor kappa-light-chain-enhancer of activated B cells; LPS, lipopolysaccharide; IL-6, interleukin-6; TMPRSS6, transmembrane serine protease 6.
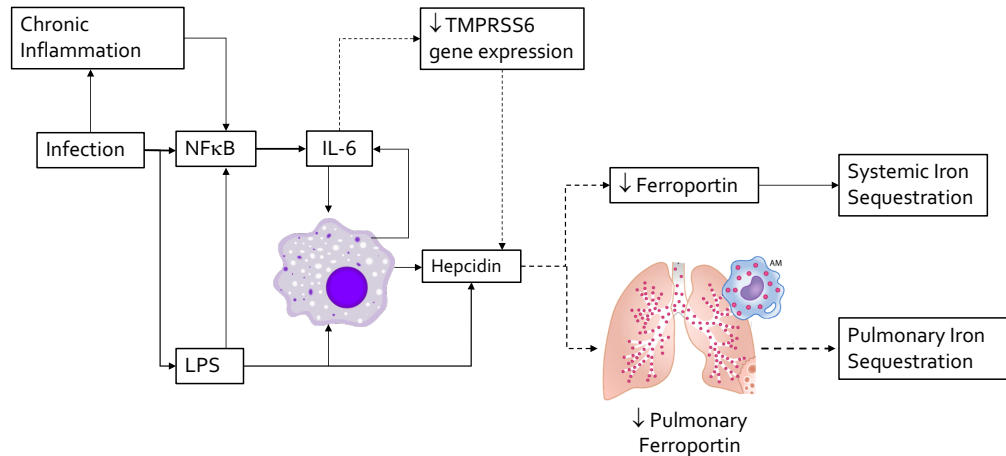
Figure 2:Interactions between infectious/inflammatory pathways and the macrophage component (best described for splenic macrophages) of the hepcidin-ferroportin axis. Dotted lines denote proposed mechanisms. Figure adapted from Cloonan et al. (2017)). NFκB, nuclear factor kappa-light-chain-enhancer of activated B cells ; LPS, lipopolysaccharide; IL-6, interleukin-6; TMPRSS6, transmembrane serine protease 6.

The Application of Sputum Iron Biomarkers in COPD

The potentially detrimental effect of increased respiratory iron to patients with COPD was seen in a retrospective study, where it was observed that a semi-quantitative measure of sputum iron, the sputum hemosiderin index (SHI), was a strong predictor of infective AECOPD (36). There was also an association between sputum IL-6 and hemosiderin, which suggests that chronic inflammation can contribute to respiratory iron. Given the limited predictors for AECOPD, the SHI could represent a simple and cost-efficient option to identify those at risk and pre-emptively intervene. Further study could

also set the stage for novel intervention strategies such as chelating iron, off-loading the left ventricle, and using monoclonal antibodies to target key pathways of pulmonary iron sequestration. To this point, the utility of sputum macrophage (SM) iron as a biomarker for recurrent infective AECOPD has not been prospectively validated, the effect of iron-overload on susceptibility to infection in the context of COPD has not been directly studied, nor have the mechanisms of respiratory iron accumulation been elucidated.

Overall Objective

To examine the role of excess airway macrophage iron on infective COPD exacerbations and potential mechanisms.

Overall Hypothesis

This thesis hypothesizes that raised respiratory iron content in COPD will increase the susceptibility to respiratory tract infection and subsequently lead to recurrent exacerbation. To test this hypothesis, specific objectives were created utilising in vitro models and a prospective observational study.

Specific Objectives

1. To establish if chronic inflammation and genetic polymorphisms contribute to the mechanisms of macrophage iron accumulation.

2. To test if increased macrophage iron content increases the susceptibility to infection with in vitro models.

3. To determine if elevated respiratory iron content is a reliable predictor of infective AECOPD in a prospective cohort.

Specific Hypotheses

This thesis hypothesizes that iron-loaded macrophages would have reduced bacterial uptake and bactericidal capacity, and chronic inflammation and genetic polymorphisms of transmembrane serine protease 6 (TMPRSS6) would contribute to iron accumulation within macrophages. For the prospective cohort, we hypothesized that individuals with an elevated SHI at baseline would have a higher frequency of infective AECOPD.

Chapter 2: General Methods and Validation Experiments

General Methods

Tamm-Horsfall Protein-1 (THP-1) Cell-Line

This human monocytic cell-line was obtained from the laboratory of Dr. Dawn Bowdish. They were maintained in RPMI 1640 (Gibco™, Gaithersburg, MD) supplemented with L-glutamine (2mM) with 10% fetal calf serum and incubated at 37°C with 5% CO_2. They were passaged weekly to keep the cellular concentration <$1x10^6$ cells/mL. A new aliquot of cells was thawed after passaging had occurred ≥12 times.

Cells were differentiated into THP-1-derived macrophages (TDM) at a concentration of $2x10^5$ cells/mL by culturing with the above media with 100nM Phorbol 12-myristate-13-acetate (PMA) for 48 hours.

Sputum Macrophage Isolation by Plastic Adherence

Sputum samples were processed as described in Chapter 5 to yield a fresh cell pellet. These were resuspended in XVivo20™ (Lonza™, Basel, Switzerland) with 5% human antibody serum and cultured in up to four, 3.5mm tissue culture plates, using one additional plate for each $1x10^7$ cells/g present in the estimated total cell count (determined by hemocytometer). These plates were placed in the incubator (37°C and 5% CO_2) overnight for 18 hours. The plates were washed with 1mL of sterile phosphate-buffered saline (PBS) twice to remove the non-adherent fraction, and subcultured in 750μL of Accutase™ (Innovative Cell Technologies, Inc., San Diego, CA) cell-

detachment solution for a further 20 minutes. After this, a cell-scraper was used to gently lift any remaining cells. An additional 750μL of cell culture media (RPMI 1640 with 10% fetal-calf serum; Gibco™, Gaithersburg, MD) was added after the adherent fraction was collected. Sputum cells were then stained with 0.4% Trypan Blue™ (Gibco™, Gaithersburg, MD) and the cells counted with a hemocytometer. A cytospin slide with hematoxylin and eosin (H&E) staining was used to confirm what proportion of cells were macrophages.

Iron Loading

Loading of macrophages was accomplished by subculturing with media containing ferrous sulphate (FeSO$_4$; ThermoFisher Scientific™, Waltham, MA) for 24-hours at concentrations of 50, 100, 250 or 500μM. Cell viability in the setting of iron loading was assessed with a PrestoBlue® assay (ThermoFisher Scientific™, Waltham, MA) at multiple time points. This Resazurin-based assay becomes fluorescent when exposed to the reducing environment of living cells, and thus increasing relative fluorescence units (RFU) within the supernatant indicates preserved cell viability.

The iron-loading protocol was validated in TDM with both the hemosiderin index and inductively-coupled plasma mass spectrometry (ICP-MS) of the cell pellet, and only with the hemosiderin index for isolated sputum macrophages (as the number of cells were too few for ICP-MS).

Iron Quantification

The hemosiderin index is a semi-quantitative measure of macrophage iron and is determined by calculating the proportion of blue-stained macrophages with Perl's Prussian Blue stain from a representative sampling of 100 macrophages under light microscopy. Further detail regarding this measure is provided in Chapter 5.

Iron concentrations were analyzed on an Agilent 8700 triple quadrupole ICP-MS™ (Santa Clara, CA). Concentrations were determined against a 13-point standard curve ranging from 0.002 µM to 4 µM. Germanium and indium were both used as internal standards and acceptable recovery rates were set at 80-120% for all measurements. At least one of the two internal standards must have met the internal standard recovery criteria for the measurement to be considered acceptable. Internal standards had a final concentration of 10 µg/L. Iron was analyzed in kinetic energy discrimination mode using two different high purity collision gases: helium and oxygen. Helium was determined to be the better gas and all results are reported with helium being the kinetic energy discrimination gas used. Each sample had a dwell time of 0.1 seconds and samples had 3 main runs per samples, each consisting of 25 sweeps. All samples were diluted 25 or 50-fold prior to analysis. Protein estimation (Protein Assay Kit II, Bio-rad™, Hercules, CA) was used to standardize the ICP-MS protocol for cell pellets after lysis with RIPA buffer (Sigma-Aldrich™, St. Louis, MO).

Statistics

For the following validation experiments, comparisons between two groups were accomplished by t-test (parametric) or Mann-Whitney test (non-parametric). Paired testing of greater than two groups was accomplished by Kruskal-Wallis test. A mixed-effects model was used to analyse the effects of incubation time and iron concentration within the media as part of the iron-loading validation experiments.

For all the data generated as part of this thesis, a P value of less than 0.05 was considered statistically significant. All analyses were performed using either SPSS 23.00. IBM Corporation, Armonk, NY, USA, or GraphPad Prism version 8.0.0 for Mac OS X, GraphPad Software, San Diego, California USA, www.graphpad.com.

Results

Iron-Loading Validation

The iron-loading protocol was first tested in TDMs and confirmed the positive effects of incubation time, and iron concentration in the media, on the hemosiderin index (both $p<0.0001$, Mixed-effects model; Figure 3). In addition, the effect of iron concentration in the media on cellular iron was confirmed by ICP-MS ($p=0.0019$, Kruskal-Wallis test; Figure 4). These two measures of macrophage iron were strongly correlated ($R^2=0.95$; Figure 5).
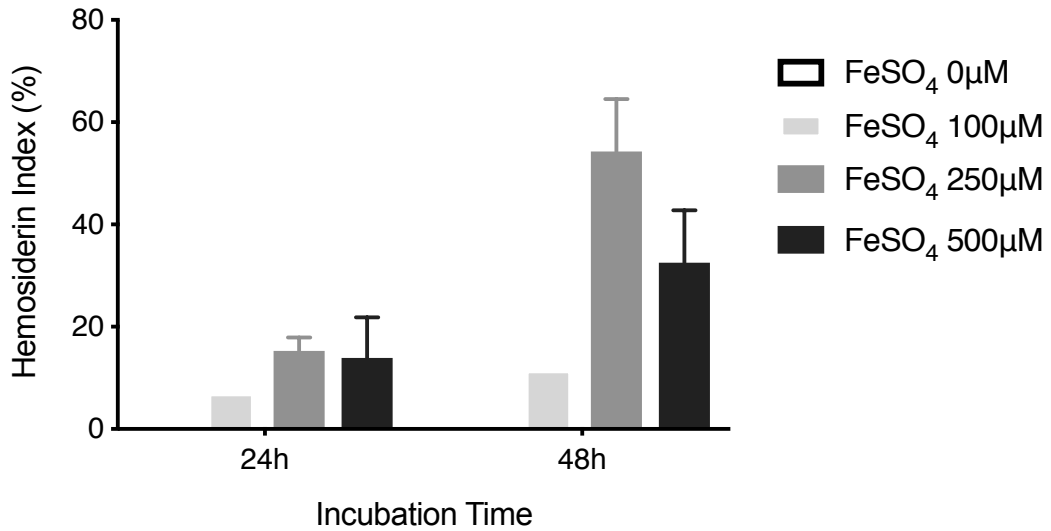
Figure 3: Cell-line-derived macrophage hemosiderin index after incubation with iron-supplemented cell-culture media. Experiments performed in duplicate (n=3).
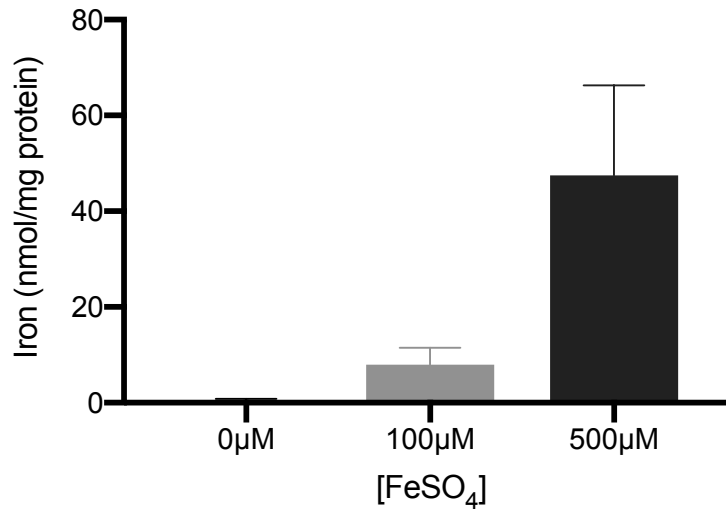
Figure 4: Iron concentration in cell-line-derived macrophages by mass spectrometry after 24-hour incubation with iron-supplemented cell-culture media. Experiments performed in duplicate (n=3).
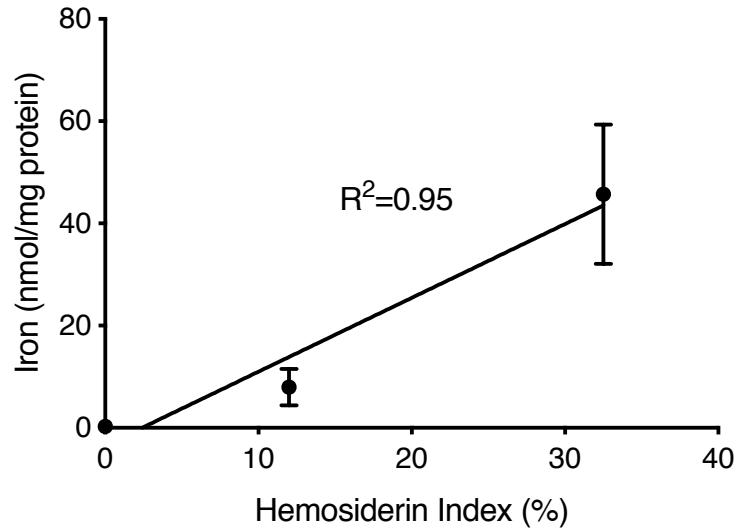
Figure 5: Linear regression of TDM hemosiderin index (%) and [Iron] standardized to concentration of protein. Experiments performed in duplicate (n=3).

In sputum macrophages, a 24-hour incubation with iron-loaded media also increased the sputum hemosiderin index significantly (Figure 6). Examples of the light microscopy images taken after incubation with iron-containing or control media are shown in Figures 7-8.
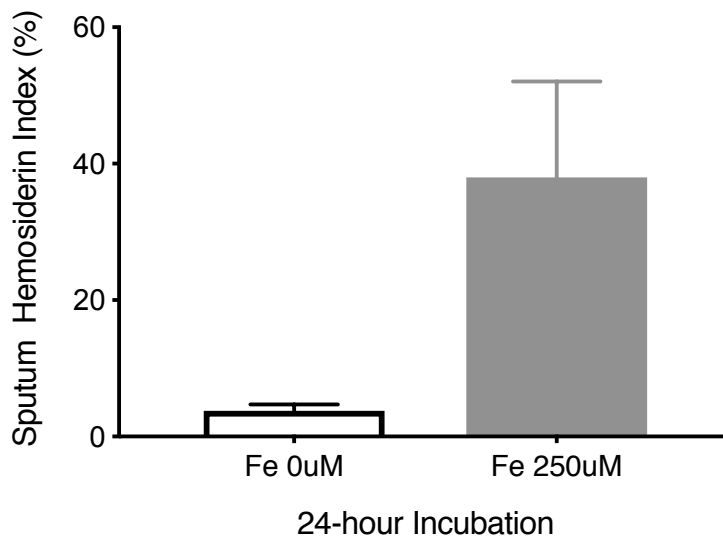
Figure 6: Sputum macrophage hemosiderin index after incubation with iron-supplemented cell-culture media. Experiments performed in duplicate (n=3).
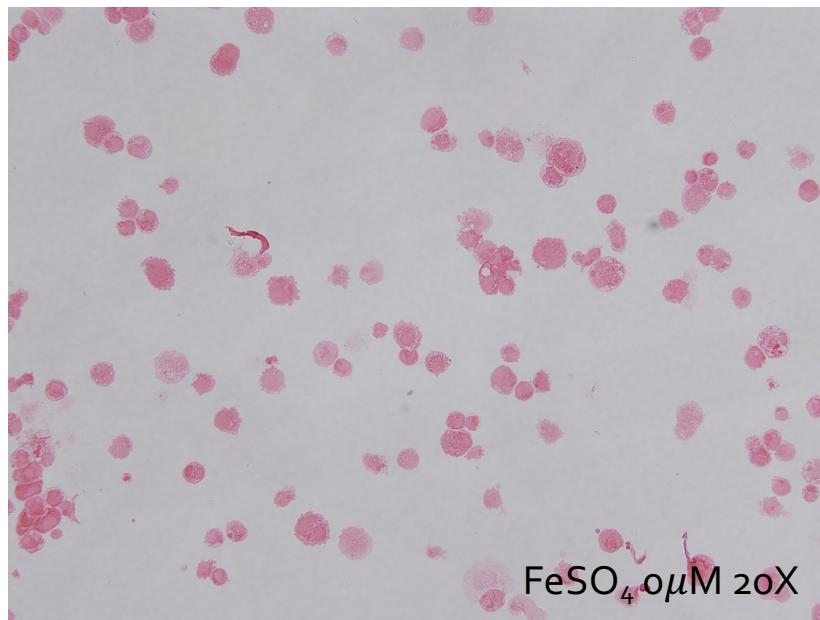
Figure 7: Light microscopy photograph of isolated sputum macrophages from healthy control. Cells cultured in control media then stained with Perl's Prussian blue.
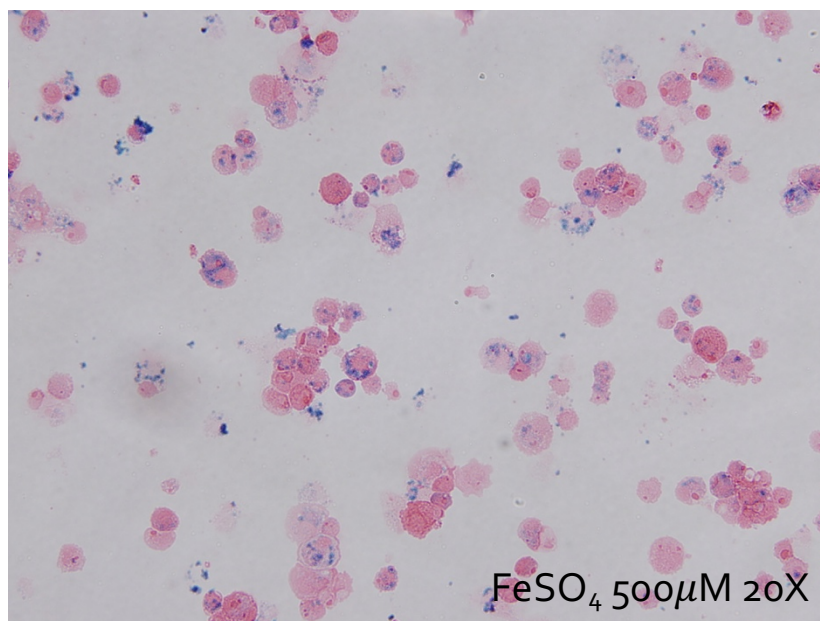
Figure 8: Light microscopy photograph of isolated sputum macrophages from healthy control. Cells treated with media containing 500μM FeSO₄ then stained with Perl's Prussian blue.

Viability of Iron-Loaded Cells

The addition of various concentrations of $FeSO_4$ did not attenuate the progressive increase in RFU (indicating cell viability) compared to control media in either TDMs or sputum macrophages (SM; Figures 9-10).
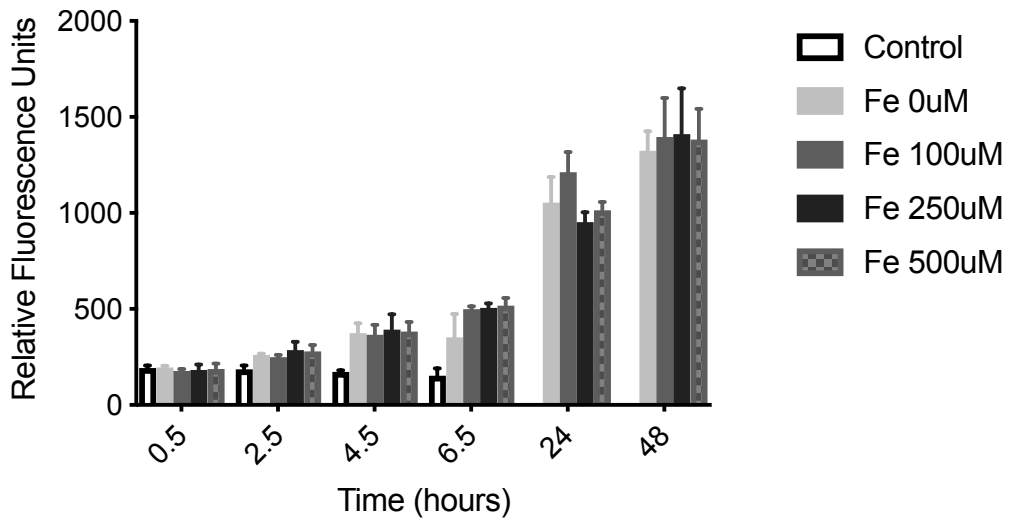
Figure 9: Viability of cell-line-derived macrophages after incubation with control and iron-loaded media. Experiments performed in duplicate (n=4)
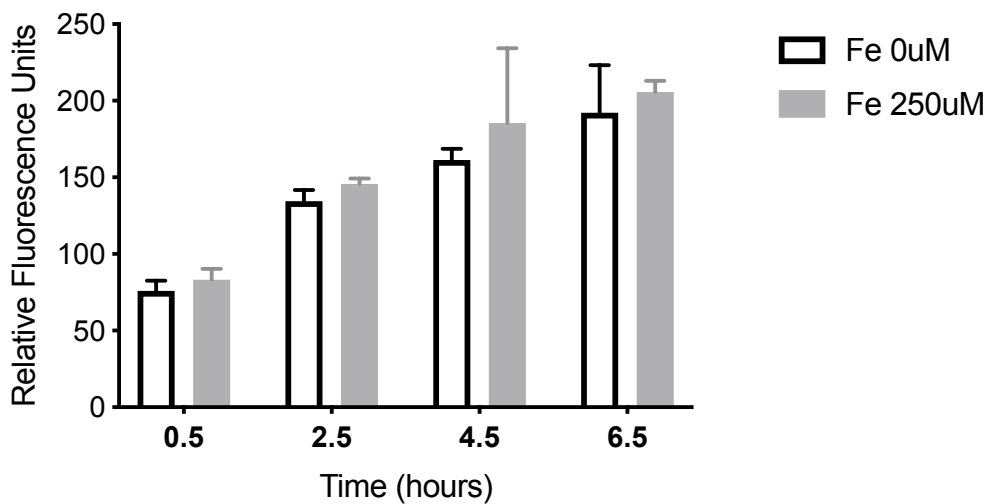
Figure 10: Viability of isolated sputum macrophages after incubation with control and iron-loaded media. Experiments performed in duplicate (n=3).

Discussion

This chapter serves as a general introduction to this thesis and describes the methods and findings related to the validation of iron-loading and viability of iron-loaded cells. Validation of these methods are important to reliably execute experiments associated with the specific objectives of this thesis. This is also the first study comparing two different measures of intracellular iron in human-derived cells.

Iron-loading of culture media led to cellular sequestration of iron in TDM and SM that followed a dose-response relationship. For TDM, this was true for both hemosiderin index and iron concentration by ICP-MS, with a strong correlation between the two measures of iron. Iron-loading was also successful in SM as confirmed by SHI. Furthermore, the addition of $FeSO_4$ to the cell culture media did not reduce the cell viability of TDM or SM as determined by a Resazurin-based assay.

Limitations of the iron-loading validation experiments include the limited time intervals used for SM viability testing. However, the viability of these cells extends at least until 30.5 hours given that these cells were subcultured in iron-containing media for 24-hours prior to starting viability testing. The cellular viability for all SM experiments (described in later chapters) was also verified with Trypan blue (Gibco™, Gaithersburg, MD) staining.

Conclusion

Intracellular macrophage iron can be experimentally increased in both TDM and SM

models, as assessed by either of two strongly correlated measures of iron: hemosiderin

index and ICP-MS. Adding iron to cell culture media did not compromise the cell

viability of TDM or SM.

Chapter 3: What are the mechanisms by which iron becomes sequestered in macrophages?

Background

Systemic versus Pulmonary Iron Homeostasis

While systemic iron homeostasis has been well described (31), less is known about iron regulation in the pulmonary system. Between these two, there are similarities and differences in the storage and regulation of iron (summarised in Table 1 (13,22,35)), but given the growing evidence supporting the importance of iron in chronic respiratory diseases, further clarification is required regarding the respiratory tract (13). There is convergence in terms of the proteins involved in uptake, extracellular binding, storage and export, but there are differences in the location of iron storage. Furthermore, the mechanisms of iron sequestration are unclear, and particularly the role of hepcidin has not been tested in human pulmonary macrophages.

	Systemic	Pulmonary
Distribution	Hemoglobin (50%), hepatocytes and Mø (25%)	Lung tissue, pulmonary Mø, airway epithelial cells
Regulation	Extracellular binding: Tf Uptake: TfR1, DMT1 Storage: Ferritin Export: FPN	Uptake: TfR1, DMT1, NRAMP1 Extracellular binding: Tf, Lactoferrin Storage: Ferritin Export: FPN
Role of Hepcidin	Degrades FPN → iron sequestration Antimicrobial (at high concentrations) Regulated by: serum iron, IL-6, BMP, TMPRSS6	Degrades FPN → iron sequestration† Antimicrobial (?) Regulated by: LPS, IL-6(?), BMP(?), TMPRSS6 (?)

Table 1: Systemic versus pulmonary iron homeostasis. † denotes conflicting evidence; (?) denotes that there is no evidence. Mø, macrophage; Tf, transferrin; TfR1, transferrin receptor-1; DMT1, divalent metal transporter-1; FPN, ferroportin; IL-6, interleukin-6; BMP, bone morphogenetic protein; TMPRSS6, transmembrane serine protease 6; NRAMP1, natural resistance-associated macrophage protein-1.

Known Sources of Pulmonary Macrophage Iron

AMs are responsible for the clearance of environmental particles, cellular debris,

including iron scavenging (11,29). As such, it comes as no surprise that in COPD lungs,

the majority of pulmonary iron is contained within AM but also in parenchymal tissue,

as demonstrated in a study of lung explants. Furthermore, in this study the quantity of

iron present was associated with the severity of airflow obstruction and emphysema

(22). Sources of pulmonary iron and luminal mechanisms of iron regulation are

summarised in Figure 11.
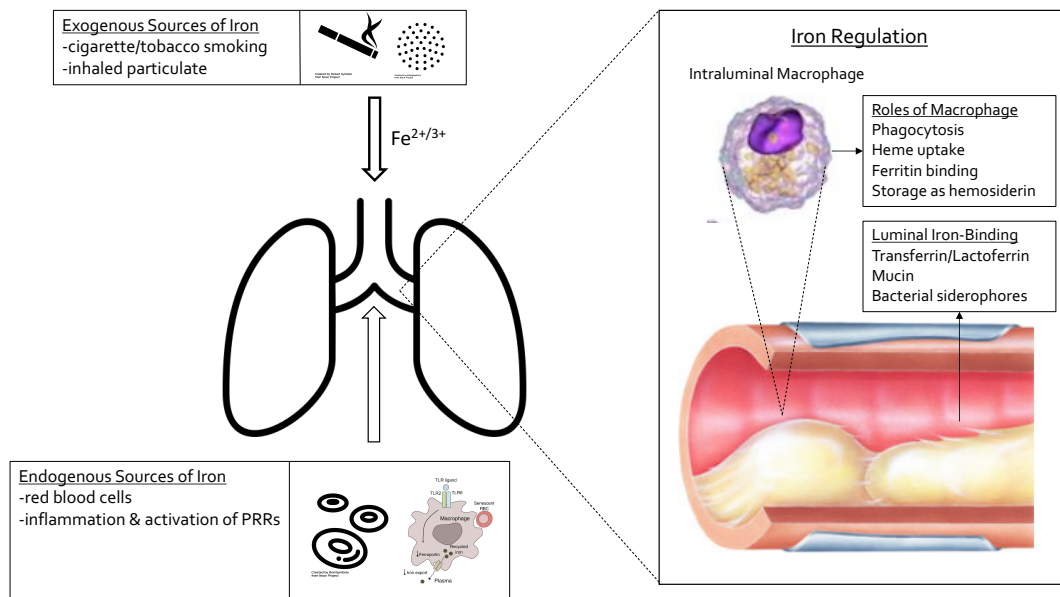
Figure 11: Potential sources of pulmonary iron and mechanisms of iron regulation in the airways. Image of toll-like receptor adapted from (37). Free images sourced from thenounproject.com and dreamstime.com.

The sources of AM iron can be exogenous, including cigarette smoke and occupational

forms of inhaled iron (32), or alternatively endogenous and related to the phagocytosis

of red-blood cells (e.g. from congestive heart failure) (30). Systemically, chronic

inflammation and genetic polymorphisms (particularly of TMPRSS6) are major contributors to iron sequestration, but their role on pulmonary macrophage iron sequestration has not been studied.

Considerations for Iron Quantification

In biological systems, iron can both exist intracellularly and extracellular, either bound or unbound to specific proteins (transferrin extracellularly and ferritin intracellularly). The measurement of extracellular iron can be accomplished through colorimetry or mass spectrometry (38,39). The measurement of intracellular iron, specifically within pulmonary macrophages, can be done semi-quantitatively by staining slides with Perl's Prussian Blue to identify iron deposits (36), or alternatively quantitatively using mass spectrometry after cell-lysis. For this thesis, iron was measured by inductively-coupled mass spectrometry after cell lysis and/or the sputum hemosiderin index after Perl's Prussian Blue stain. This would allow for accurate quantification of total iron (after protein-bound iron had been released), comparison of these two measurement techniques, and subsequent validation of SHI for potential clinical use.

Mechanisms of Systemic Iron Sequestration

To effectively test the mechanisms of pulmonary iron sequestration, an understanding of the mechanisms of systemic iron homeostasis is required. As previously mentioned, hepcidin is the most important protein in iron homeostasis and enacts its effects

through the degradation of ferroportin. It is produced predominantly by the liver in response to inflammatory stimuli, and its expression is inhibited by low systemic and hepatic iron levels, and hypoxia of hepatocytes (31). It is also produced by macrophages, epithelial cells, and dendritic cells (40), though its role when secreted from these cells is less clear (41).

There are two main mechanisms by which hepcidin is secreted from hepatocytes, via IL-6 and the Janus kinase (JAK) signal transducer and activator of transcription (STAT) 3 pathway, or alternatively indirectly via the TMPRSS6 gene by way of the bone morphogenetic protein-Smad (BMP-Smad) and STAT5 pathways (31). Splenic macrophages behave similarly to hepatocytes in response to IL-6 with the added effect that autocrine and paracrine production of IL-6 occurs (Figure 2). They can also release hepcidin directly in response to activation of pattern recognition receptors (PRR; (41).

The TMPRSS6 gene encodes for the transmembrane serine protease, matriptase-2, which negatively regulates hepcidin. It is most highly expressed in hepatocytes, but is also present in lung tissue (42). In a normal individual, matriptase-2-mediated tonic inhibition of hepcidin prevents excessive iron sequestration. However, in the case of a common genetic polymorphism to this gene, rs855791, the inhibition of hepcidin is amplified, which effectively shunts the control of iron sequestration to IL-6 (Figure 12). Therefore, if this polymorphism is present concurrently with chronic inflammation, iron

sequestration is more likely to occur (43). This genetic polymorphism is common, with

prevalence estimated at >85% of individuals (43).
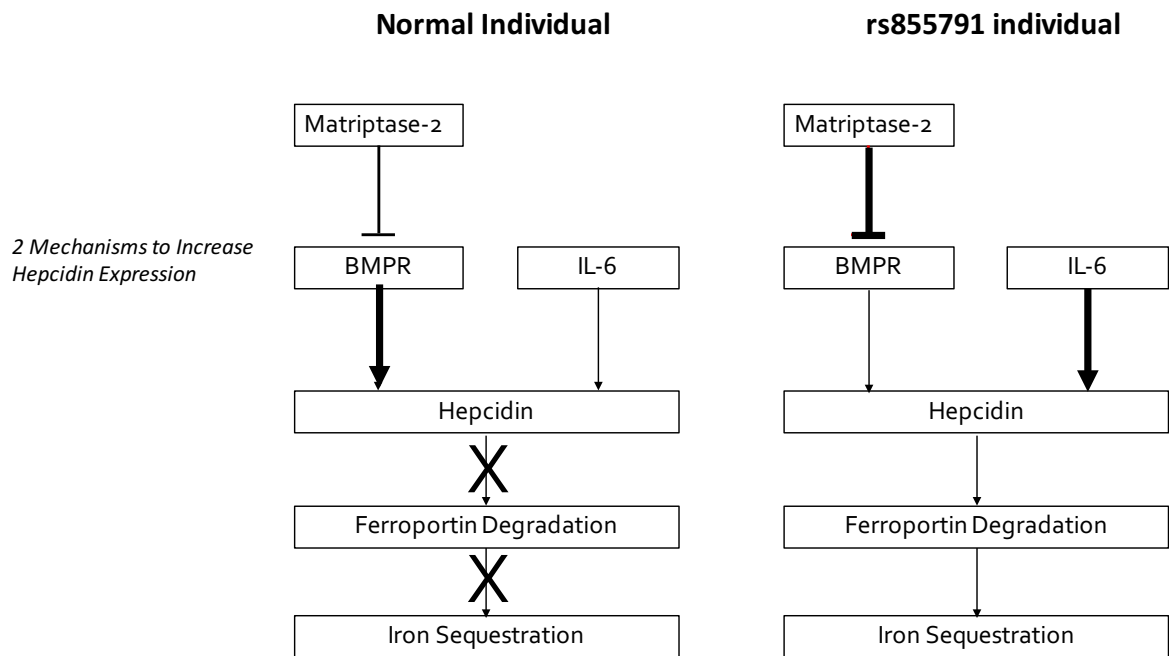
Figure 12: Conceptual diagram of hepcidin control in normal individuals and those with rs855791 polymorphism. BMPR, bone morphogenetic protein receptor; IL-6, interleukin-6.

Interaction between Infection and the Hepcidin-Ferroportin Axis

The mechanisms underlying the release of hepcidin from hepatocytes in response to

infection are well characterised in animal models. These studies confirmed that a

variety of stimuli are able to activate PRRs on macrophages, leading to NFκB-mediated

release of IL-6, which upon contacting hepatocytes, results in the systemic release of

hepcidin (31,41). An alternative mechanism resulting in hepatic release of hepcidin was

recently described and related to the downregulation of TMPRSS6 gene expression by

IL-6 (39).

Experimental macrophage models have demonstrated that these cells also release

hepcidin in response to IL-6. However, it is not clear if macrophage-derived hepcidin

contributes to systemic iron homeostasis, though it is plausible that it could prevent the

release of scavenged iron (related to autocrine activity) (41). Evidence from human cell-

line-derived macrophages demonstrated that hepcidin was directly stimulated by non-

tuberculous-mycobacterial infection most strongly in the presence of Interferon-γ, and

also with IL-6 (44). However, tuberculosis mouse-models have had conflicting results in

terms of hepcidin gene expression in macrophages (40,45). Therefore, it appears that

hepcidin release from macrophages is microbe-dependent, with more evidence for

intracellular organisms (41). In addition, there is evidence that the release of hepcidin by

infection could be mediated by toll-like receptors (TLR), and that iron sequestration in

macrophages could even occur by hepcidin-independent mechanisms. These authors

used TLR-ligands and experimental Listeria infection to demonstrate one hepcidin-

dependent and one hepcidin-independent mechanism by which ferroportin was

downregulated (46).

The effect of hepcidin on subsequent infection has been studied to a lesser degree.

Exogenous hepcidin increased cytosolic iron but impaired the generation of ROS in

Salmonella-infected murine macrophages, highlighting a possible mechanism by which

susceptibility to infection can be impacted by this axis (47). In another study, hepcidin

knockout mice did not have an increased mycobacterial load (45), but the effect of excess hepcidin has not been studied.

If infection-mediated hepcidin release leads to intracellular iron-loading through the hepcidin-ferroportin axis, and iron-overload predisposes to infection, this could form the basis of a cycle of recurrent infection facilitated by hepcidin's involvement in both inflammation and iron regulation.

Mechanisms of Pulmonary Iron Sequestration

Ex vivo studies of healthy controls and mouse models have confirmed that AMs express hepcidin, and that IL-6-receptors are present on AMs, but it is unclear if this pathway is responsible for iron sequestration in lung macrophages (35,48). While murine AMs treated with hepcidin or lipopolysaccharide (LPS) experience downregulation of ferroportin, this has not been explicitly linked to iron sequestration (35). Furthermore, there has been only a single experiment examining human lung macrophages (48).

The effect of pulmonary hepcidin was tested in mice with complete and liver-specific hepcidin knockout. This study revealed a similar amount of pulmonary iron in both types of mice, suggesting that pulmonary hepcidin could be redundant in iron regulation (49). They also found that intranasal but not intra-peritoneal LPS upregulated hepcidin release without changing pulmonary iron content (49).

In-vitro experiments demonstrated that Interferon-γ and IL-6 both induced hepcidin expression in airway epithelial cells from healthy controls, but exogenous hepcidin did not reduce ferroportin expression in these cells (48).

To summarise, the mechanisms behind pulmonary iron sequestration are poorly understood, with evidence almost exclusively from murine models. A single study has examined human respiratory tract cells, but focused on airway epithelial cells rather than pulmonary macrophages. This objective will test the effect of key cytokines/proteins on iron sequestration in human sputum macrophages with ex vivo experiments, and determine if there is evidence for these potential mechanisms in a cohort of COPD patients.

Methods

<u>Cytokine/Protein Assays</u>

IL-6 (R&D Systems™, Minneapolis, MN) and hepcidin (R&D Systems™, Minneapolis, MN) were quantified by enzyme-linked immunosorbent assay (ELISA). Lower limits of detection were 9.38 pg/mL and 3.12 pg/mL, respectively. Both ELISAs were performed following the user's manual with substitution of Strepavidin alkaline phosphatase rather than the Strepavidin horseradish peroxidase provided in the kits. For the IL-6 assay, sputum supernatant samples were diluted 1:1, while no dilution was used for other

sample types (including serum and cell-line supernatant). For the hepcidin assay,

sputum and cell-line supernatant samples were not diluted, while serum samples were

diluted 1:500. Plates were read on a Spectramax™ plate reader using Softmax Pro

Software™. Concentrations were calculated by interpolation from a sigmoidal standard

curve.

RNA Extraction and Real-time Quantitative Polymerase Chain Reaction

Messenger ribonucleic acid (mRNA) was isolated from frozen cell pellets (previously

stored at -80ºC in 90% fetal calf serum [Invitrogen™, Carlsbad, CA] and 10% dimethyl

sulfoxide freezing media [Sigma-Aldrich™, St. Louis, MO]) from eight COPD subjects (4

with SHI<10 and 4 with SHI≥10), and 3 healthy controls by magnetic microbeads

(μMACS™ mRNA isolation kit, Miltenyi™, Bergisch Gladbach, Germany), then reverse-

transcribed to create complementary deoxyribonucleic acid (cDNA; μMACS™ cDNA kit,

Miltenyi™™, Bergisch Gladbach, Germany), and stored at -80ºC. Nanodrop™ One

(ThermoFisher Scientific™, Waltham, MA) was used to quantify the concentration of

cDNA present. Expression levels of human hepcidin antimicrobial peptide (HAMP),

ferroportin (SLC40A1) and TMPRSS6 genes were reported to those of GAPDH

housekeeping gene. The primer sequences were as follows: human hepcidin:

CTGCTGCGGCTGCTGTCATCGATCAAAGTGTGGGATGTGCTGCAAGACGTAGAACCTA

CCTGCCCTGCCCCCGTCCCCTCCCTTCCTTATTTATTCCTGCTGCCCCAGAACATAGGTC

T; human ferroportin: GTAGGAGACCCATCCATCTCGGAAGGTACGGAAGGGCTCAGC

CATCTGGGAGGCACAAGTAGGCTCTTGCTCATGTTCAAGCTCATGGATGTTAGAGTCTT

TCACACCCATTAG; human TMPRSS6: CCAAAGGAATAGACGGAGCTGGAGTTGTA

GTAAGTTCCCAGGCGGGTGCTGGTGATGAGCTCCTTGAGCATCTTCTGGGCTTTGGCG

GTTTCACTGCGGAAGGCACTAGATTCCCGGCGGGTAAGATCCTGGGAGAAGTGGCGAT

TGAGTACACGCAGACTGCCTGAGTACACCTGG; and human GAPDH: GTATGACAA

CGAATTTGGCTACAGCAACAGGGTGGTGGACCTCATGGCCCACATGGCCTCCAAGGAG

TAAGACCCCTGGACCACCAGCCCCAGCAAGAGCACAAGAGGAAGAGAGAGACCCTCA

CTGCTGGGGAGTCCCTGCCACAC. Synthetic templates for the genes of interest were

used as positive controls. All primers and synthetic templates were purchased from Bio-

rad™ (Hercules, CA).

A QuantStudio3™ (ThermoFisher Scientific™, Waltham, MA) machine and its

corresponding software were used to complete the reactions as per the suggested

protocol (as per kit instructions) and analyse the results. Each sample was plated in

triplicate. Briefly, in each well (of a 96-well plate), 3μL of sample cDNA was added to

1μL of primer, 10μL of SYBR green supermix (Bio-rad™, Hercules, CA), and 6μL of

nuclease-free water. The cycling protocol involved an activation step (95°C for 2

minutes) and then forty cycles of denaturation and annealing (95 °C for 5 seconds, then

60°C for 30 seconds for each cycle).

The difference in cycle threshold (ΔCt) for each gene of interest was calculated by subtracting Ct for GAPDH from that of the gene of interest (ΔCt = Ct_{gene} - Ct_{GAPDH}). To determine the relative expression in COPD subjects, the ΔCt for the gene of interest in these subjects was compared to the average ΔCt in healthy controls. Given a reaction efficiency of two, relative expression was calculated as follows:

$$Relative\ Expression = \frac{2^{\Delta Ct}COPD}{2^{\Delta Ct}Healthy}$$

TMPRSS6 Genotype

The presence of rs855791, a genetic polymorphism of TMPRSS6, was identified by sequence allele specific PCR from cDNA that was reverse-transcribed from whole blood mRNA samples that had been collected from patients and saved in PAXGene™ tubes (PreAnalytix™, Feldbachstrasse, Switzerland) at -80ºC. These samples were processed by a collaborator.

Mechanisms of Iron Sequestration (TDM)

THP-1 cells with PMA at a concentration of 2.5×10^6 cells/mL were pipetted into a 24-well plate and allowed to differentiate over 48 hours. The plate was then centrifuged, supernatant aspirated, and tested conditions plated in duplicate. Each condition was combined with media containing $FeSO_4$ 100µM and included: heat-inactivated HI (1×10^6 bacteria in 35µL PBS; hi-HI), recombinant human IL-6 at 50 ng/mL (Abcam™,

Cambridge, UK), recombinant human hepcidin at 1µg/mL (Peptides International™, Louisville, KY), hi-HI with IL-6, hi-HI with hepcidin, IL-6 with hepcidin, and hi-HI with IL-6 and hepcidin. Heat inactivation of HI was achieved by incubating at 55°C for 10 minutes. Cells were subcultured under these conditions for 24-hours, after which the plate was centrifuged, and the supernatant aspirated and stored at -20°C. After the supernatant was completely aspirated, each well was washed with 2mL of PBS, and then incubated with 0.5mL of 0.25% trypsin (Gibco™, Gaithersburg, MD) to lift the cells. An additional 0.5mL of RPMI 1640 (Gibco™, Gaithersburg, MD) supplemented with L-glutamine (2mM) with 10% fetal calf serum was then added and 10µL used to count cells and test viability. A portion of the cell-suspension was used for a hemosiderin slide and the remaining saved as a cell pellet.

The primary outcome of this experiment was intracellular iron content by ICP-MS. Secondary outcomes included macrophage iron efflux, cell-pellet iron hemosiderin index, and IL-6 and hepcidin concentrations (by ELISA) in the supernatant. Iron efflux was calculated indirectly by subtracting the iron concentration of control media from that of the supernatant after 24-hours of incubation. A reduction in concentration indicates that iron was taken up by one of the iron importers, but prevented release due to reduced ferroportin.

<u>Mechanisms of Iron Sequestration (Sputum Macrophages)</u>

Sputum macrophages were isolated from healthy controls (non-smokers without a history of a chronic respiratory condition) as described in the Methods of Chapter 1. The protocol was identical to that used for TDM (as above) except cells were divided into 3.5cm dishes for each of three conditions: iron alone, iron with IL-6 at 50 ng/mL (Abcam™, Cambridge, UK), or iron with hepcidin at 1μg/mL (Peptides International™). Fewer conditions were applied due to the smaller yield of cells compared to the cell-line experiments. Cells were lifted in a similar fashion as per the TDMs, but with Accutase™ (Sigma-Aldrich™, St. Louis, MO) rather than trypsin, and a cell-scraper. The primary outcome for SM was macrophage iron efflux due to the smaller yield of cells.

Prospective Cohort

The mechanisms of pulmonary iron sequestration were also tested in a cohort of COPD patients utilised for Objective 3 (as described in the Methods of Chapter 5). These subjects had their serum and cell-free sputum supernatant samples at the time of AECOPD and during clinical stability tested for IL-6 and hepcidin concentrations by ELISA. These were used to determine if SHI correlated with IL-6 and/or hepcidin, and to test if IL-6 status and TMPRSS6 polymorphism conjointly affected SHI.

Statistics

For the macrophage experiments, comparisons between the control group and conditions were performed by ANOVA (with Dunnett's multiple comparisons test) for

parametric data and Kruskal-Wallis tests (with Dunn's multiple comparisons test) for non-parametric data. Group comparisons of grouped data were accomplished by Friedman test.

For the prospective cohort data, descriptive statistics are presented as median (IQR) due to the non-parametric nature of the data. Data from IL-6 and hepcidin ELISA were log-transformed for graphical purposes. Linear regression and Spearman correlations were used to determine the associations between IL-6 and hepcidin with SHI. Mann-Whitney test was used to compare two groups for non-parametric data.

Results

TDM Experiments

Iron Efflux

The difference between the iron measured in the control media and each condition after 24 hours was measured as a relative reduction (%). There was a significant difference between the tested conditions and control (p=0.022, ANOVA). Multiple comparisons testing further revealed significant reductions in the following groups: IL-6 ($-21.6\pm5.09\%$, p=0.028), hepcidin ($-19.7\pm8.59\%$, p=0.04), hi-HI ($-22.3\pm4.92\%$, p=0.023), IL-6 and hi-HI ($-20.5\pm6.43\%$, p=0.038), and hepcidin and hi-HI ($-27.8\pm2.75\%$, p=0.0052, all by Dunnett's multiple comparisons test; Figure 13).
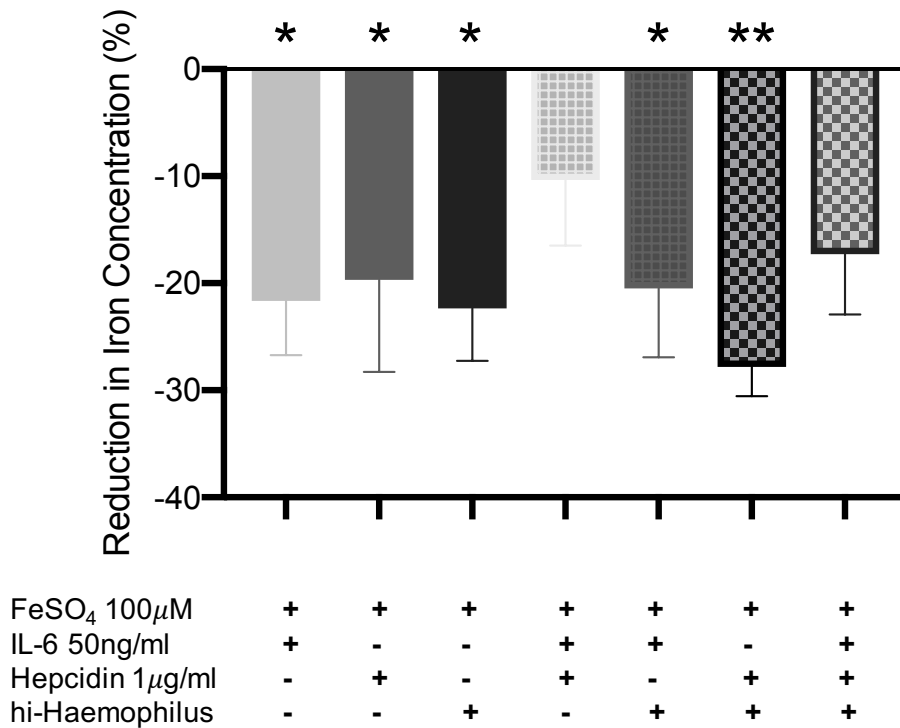
*Figure 13: Reduction in supernatant iron concentration after 24-hour incubation of condition with cell-line-derived macrophages (relative to control). Data presented as mean±SD. Experiments performed in duplicate (n=5). * denotes p<0.05, ** denotes p<0.01. FeSO$_4$, ferrous sulphate; IL-6, interleukin-6; hi, heat-inactivated.*

Cellular Iron Quantification

Compared to control (median 0 [0,1.00]%), the hemosiderin index increased significantly when TDM were subcultured with the various conditions (p=0.0379, Kruskal-Wallis test; Figure 14). Multiple comparisons testing demonstrated that IL-6 and Hepcidin together (median 21.0 [13.0,31.0] %, p=0.0089, Dunn's multiple comparisons test) led to a significant sequestration of iron. Unexpectedly, hi-HI being present with IL-6 and/or Hepcidin led to a non-significant degree of iron sequestration.
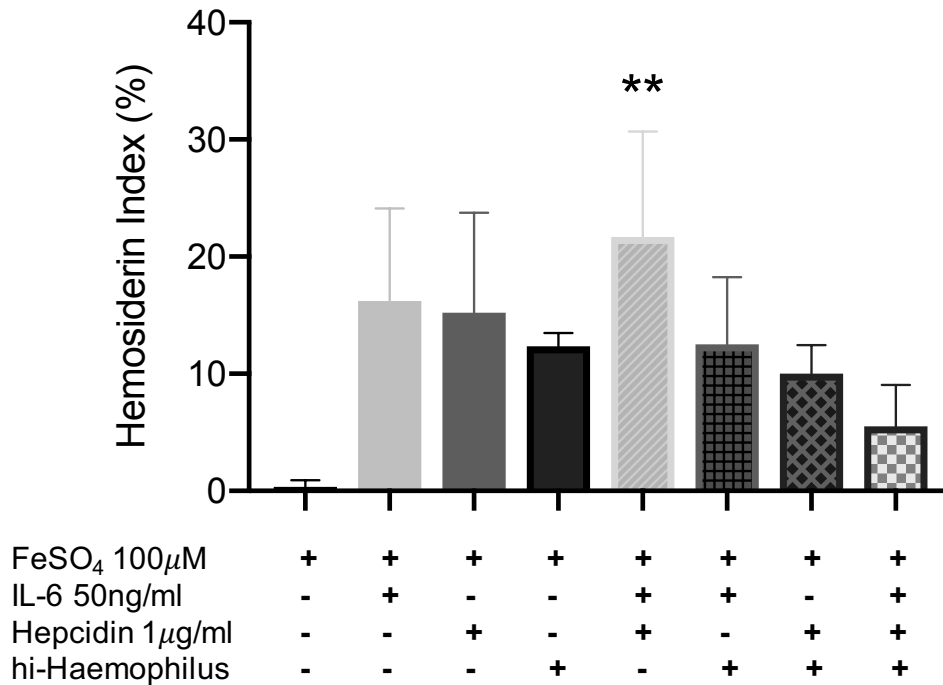
Figure 14: Hemosiderin index of cell-line derived macrophages after 24-hour incubation with various conditions. Data presented as median (IQR). Experiments performed in duplicate (n=5). ** denotes p<0.01. FeSO4, ferrous sulphate; IL-6, interleukin-6; hi, heat-inactivated.

The iron content as calculated by ICP-MS behaved similarly, showing increased iron compared to control (median 2.00 [0.671,2.99] μM) when TDM were subcultured with the various conditions (p=0.009, Kruskal-Wallis test). Multiple comparisons testing demonstrated that IL-6 (median 16.0 [12.4,18.0] μM, p=0.014), Hepcidin (median 17.2 [15.2,18.8] μM, p=0.0028), and IL-6 and Hepcidin (median 17.6 [9.71,20.9] μM, p=0.014, all by Dunn's multiple comparisons test; Figure 15) led to a significant sequestration of iron.
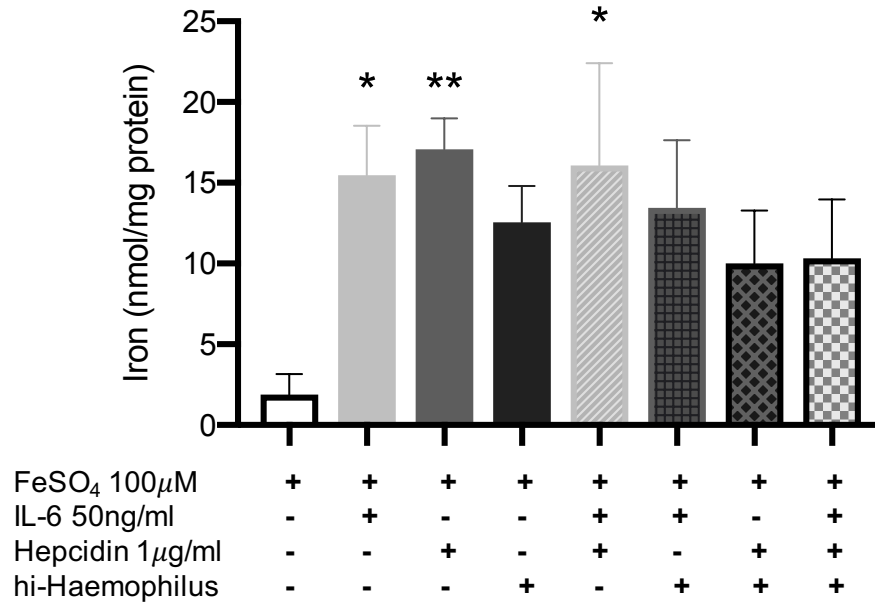
*Figure 15: Intracellular iron content (by mass spectrometry) of cell-line derived macrophages after 24-hour incubation with various conditions. Data presented as median (IQR). Experiments performed in duplicate (n=5). * denotes p<0.05, ** denotes p<0.01. FeSO₄, ferrous sulphate; IL-6, interleukin-6; HI, heat-inactivated.*

IL-6 and Hepcidin ELISA

These secondary outcomes were measured to confirm the mechanism by which chronic inflammation interacts with the hepcidin-ferroportin axis. There was a difference between test conditions and the control group (media with iron; p<0.0001, ANOVA). Multiple comparisons testing revealed that compared to the control condition, IL-6 absorbance increased in the hi-HI (p<0.0001), and hepcidin with hi-HI (p<0.0001) conditions. Furthermore, the hepcidin and hi-HI group had higher secretion of IL-6 than the hi-HI group alone (p=0.0002; all by Dunnett's multiple comparisons test; Figure 16) conditions.
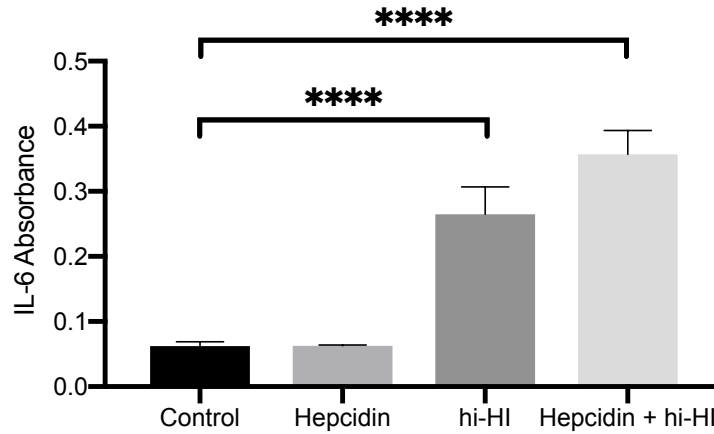
Figure 16: Interleukin-6 ELISA absorbance values in cell-line-derived macrophages after 24-hour incubation with various conditions. Data presented as mean±SD. Experiments performed in duplicate (n=5). **** denotes p<0.0001. IL-6, interleukin-6; hi-HI, heat-inactivated Haemophilius influenzae.

For hepcidin absorbance levels, there was a trend towards a difference between the control group and the test conditions (p=0.0502, Kruskal-Wallis). With multiple comparisons testing, it was demonstrated that the IL-6 with hi-HI condition had a significant increase in hepcidin absorbance (p=0.0498, Dunn's multiple comparisons test; Figure 17).
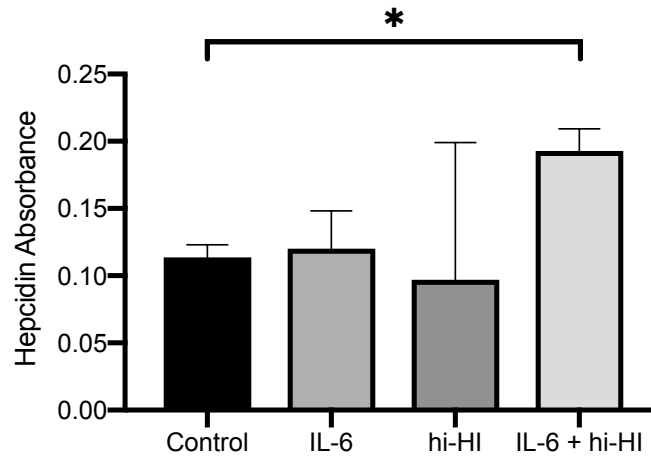
Figure 17: Hepcidin ELISA absorbance values in cell-line-derived macrophages after 24-hour incubation with various conditions. Data presented as median (IQR). Experiments performed in duplicate (n=5). * denotes p<0.05. IL-6, interleukin-6; hi-HI, heat-inactivated Haemophilius influenzae.

Sputum Macrophage Experiments

Iron Efflux

Between the two tested conditions (IL-6 and hepcidin-treated), there was a trend

towards a difference in iron concentration as determined by ICP-MS (p=0.069,

Friedman test). Multiple comparisons testing revealed near-significant reductions in IL-

6-treated (-21.8 [-17.8,-26.2] %, p=0.068) and hepcidin-treated sputum macrophages

compared to control (-19.6 [-9.68,-21.9] %, p=0.068, both by Dunn's multiple

comparisons test; Figure 18).
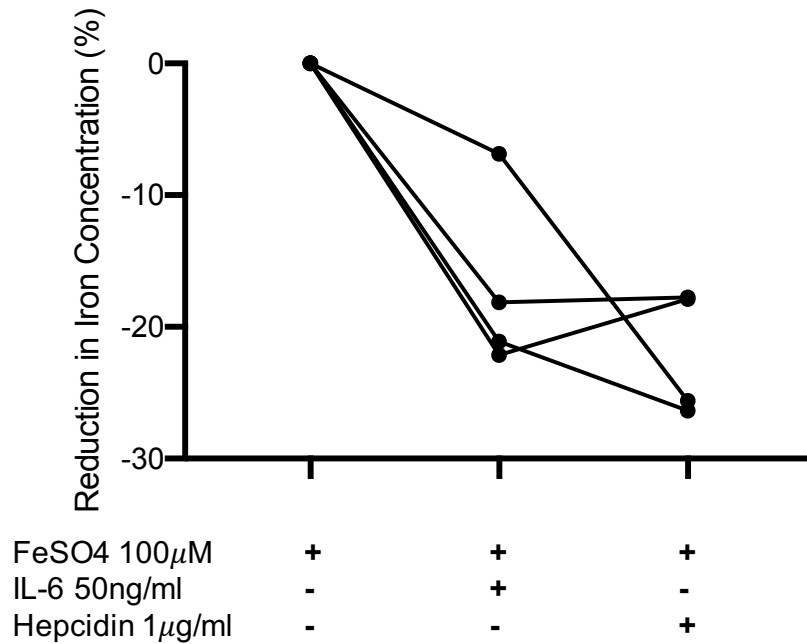
Figure 18: Reduction in supernatant iron concentration after 24-hour incubation of condition with isolated sputum macrophages. Data presented as mean±SD. FeSO$_4$, ferrous sulphate; IL-6, interleukin-6.

IL-6 and Hepcidin from Prospective Cohort

Baseline characteristics and sputum iron measures of the 49 subjects enrolled in the prospective cohort are available in Tables 2-4 and Figures 39-40, respectively in Chapter 5. Only six subjects did not have a TMPRSS6 genetic polymorphism, which is not unexpected in a predominantly Caucasian population (43).

Serum IL-6 was not significantly different at AECOPD (median 3.36 [2.24,10.7] pg/mL) and at follow-up (median 2.78 [2.30,36.6] pg/mL; Figure 19). Sputum IL-6 also did not demonstrate a significant difference at AECOPD (median 63.4 [11.5,211] pg/mL) and during follow-up (median 111 [34.2,198] pg/mL; Figure 20).
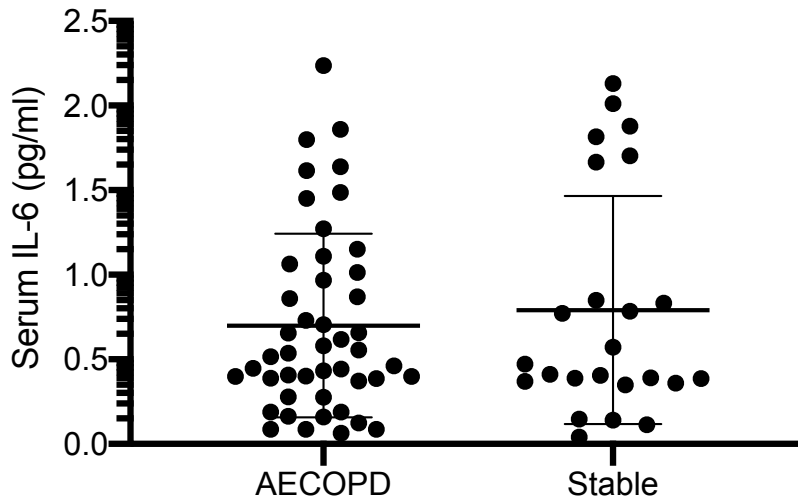
Figure 19: Serum interleukin-6 levels (as measured by ELISA) in chronic obstructive pulmonary disease cohort during exacerbation and clinical stability. Data log-transformed and presented as mean±SD. IL-6, interleukin-6; AECOPD, acute exacerbation of COPD.
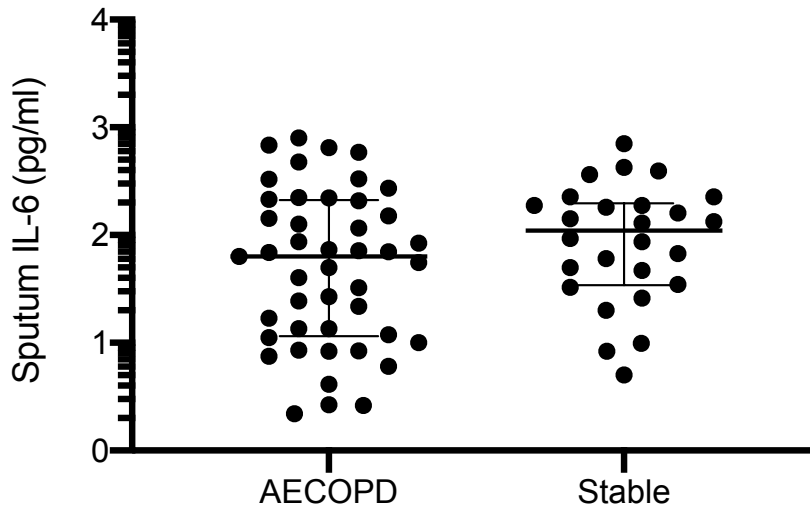
Figure 20: Sputum supernatant interleukin-6 levels (as measured by ELISA) in chronic obstructive pulmonary disease cohort during exacerbation and clinical stability. Data log-transformed and presented as mean±SD. IL-6, interleukin-6; AECOPD, acute exacerbation of COPD.

Serum hepcidin was significantly higher during AECOPD (median 77800 [18900,111000]

pg/mL) than during follow-up (median 24800 [4590,79600] pg/mL; Figure 21). Sputum

hepcidin did not demonstrate a significant difference at AECOPD (median 31.1

[11.5,211] pg/mL) and during follow-up (median 111 [34.2,198] pg/mL; Figure 22).
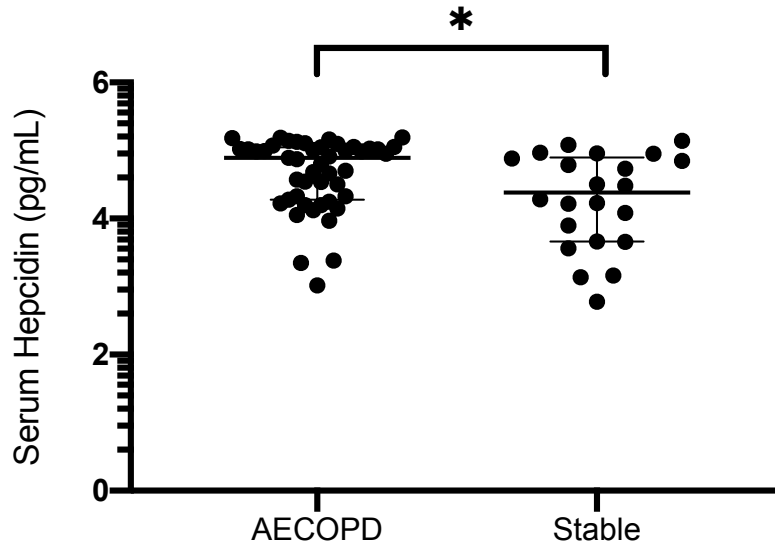
*Figure 21: Serum hepcidin levels (as measured by ELISA) in chronic obstructive pulmonary disease cohort during exacerbation and clinical stability. Data log-transformed and presented as mean±SD. * denotes p<0.05. AECOPD, acute exacerbation of COPD.*
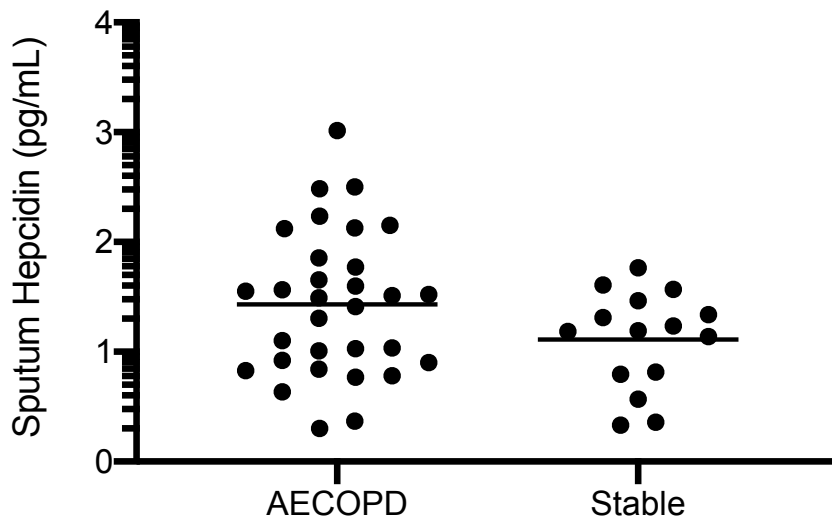
Figure 22: Sputum supernatant hepcidin levels (as measured by ELISA) in chronic obstructive pulmonary disease cohort during exacerbation and clinical stability. Data log-transformed and presented as mean±SD. AECOPD, acute exacerbation of COPD.

Correlations between serum IL-6 and serum or sputum hepcidin were examined to determine if there was population-level evidence that IL-6 led to the upregulation of hepcidin systemically and/or locally in the airway. Linear regression between serum IL-6 and serum hepcidin revealed a significant association (r=0.31, p=0.0418). No significant associations were seen between serum IL-6 and sputum hepcidin, and sputum IL-6 and sputum hepcidin.

There was no correlation between SHI at AECOPD with serum or sputum levels of IL-6 or hepcidin. However, SHI at follow-up was correlated with sputum (r=0.37, p=0.045, Spearman; Linear regression shown in Figure 23) and serum IL-6 (r=0.31, p=0.086, Spearman; Linear regression shown in Figure 24) measured during AECOPD.
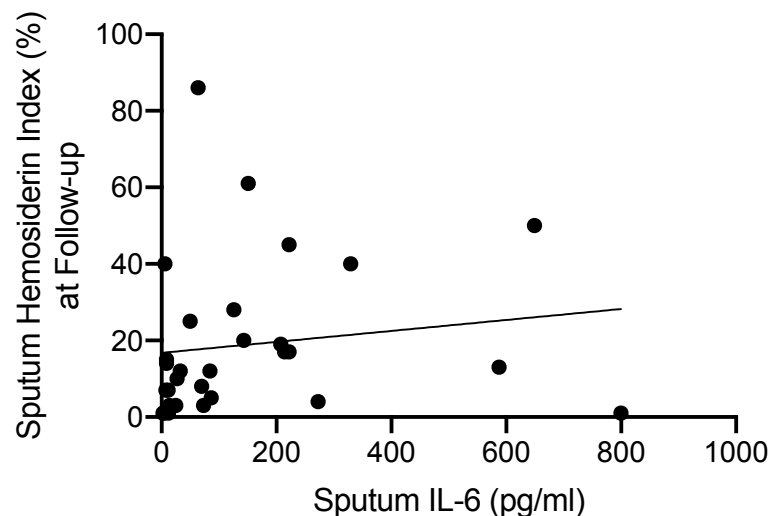
Figure 23: Linear regression of sputum supernatant interleukin-6 (by ELISA) and sputum hemosiderin index. IL-6, interleukin 6.
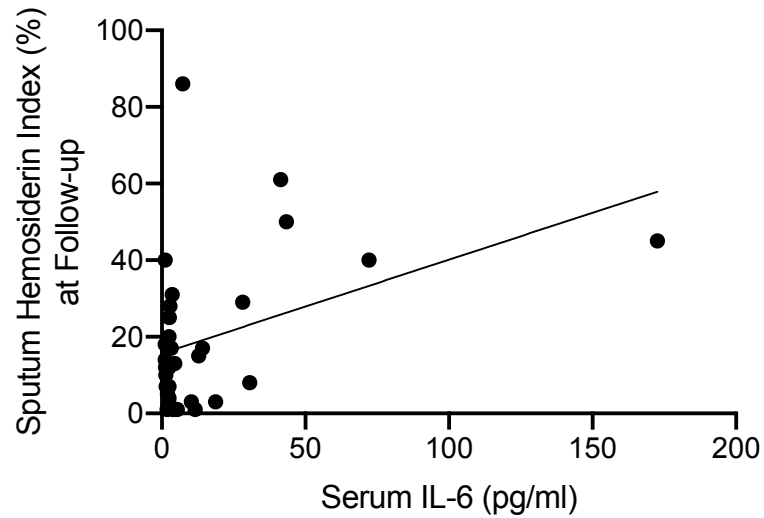
Figure 24: Linear regression of serum interleukin-6 (by ELISA) and sputum hemosiderin index. IL-6, interleukin 6.

The effect of IL-6 in the presence of the TMPRSS6 single-nucleotide polymorphism (SNP) on SHI was tested by grouping subjects with this polymorphism by IL-6 status at follow-up (in the sputum defined by the median level; in the serum defined by a threshold level 4 pg/mL). The SNP$^+$SpIL-6^{hi} had a higher sputum macrophage iron compared to the SNP$^+$SpIL-6^{lo} group (Figure 25). The low number of subjects who were negative for TMPRSS6 SNP prevented robust statistical analysis, though when stratifying by sputum IL-6, the SNP$^-$ group had a SHI approaching that of SNP$^+$SpIL-6^{lo} group (data not shown). When stratifying by serum IL-6, there was a trend towards the SNP$^+$SeIL-6^{lo} group having a lower SHI compared to the SNP$^+$SeIL-6^{hi} group (Figure 26).
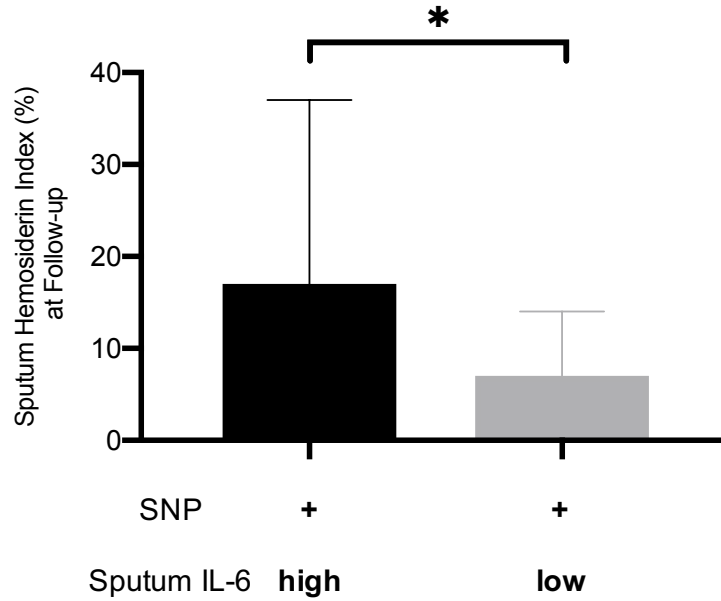
Figure 25: Effect of sputum supernatant IL-6 status on sputum hemosiderin index in SNP[+] chronic obstructive pulmonary disease patients. Data presented as median (IQR). SNP, single nucleotide polymorphism of TMPRSS6; IL-6, interleukin 6.
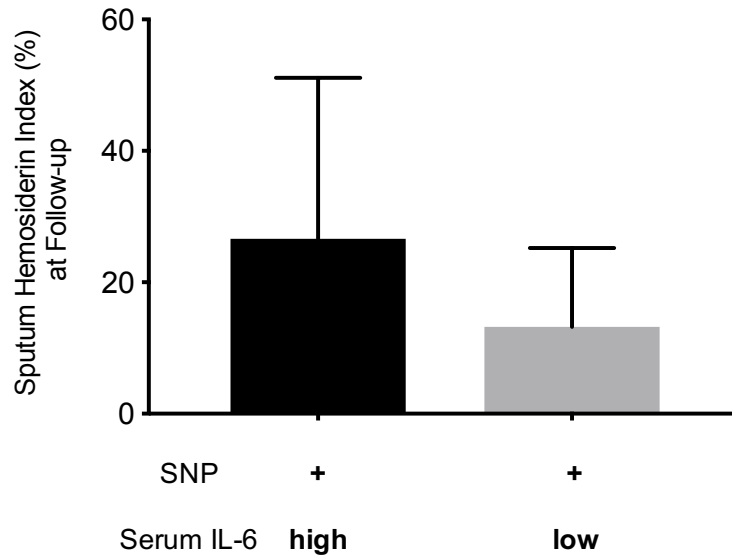
Figure 26: Effect of serum IL-6 status on sputum hemosiderin index in SNP[+] chronic obstructive pulmonary disease patients. Data presented as median (IQR). SNP, single nucleotide polymorphism of TMPRSS6; IL-6, interleukin 6.

Real Time Quantitative Polymerase Chain Reaction (RT-qPCR)

The low SHI group had indices of 1, 3, 4 and 8, while the high SHI group had indices of 20, 45, 53, and 64. There was no differences in the expression of HAMP (relative to healthy controls) between SHI[lo] and SHI[hi] (p=0.89, Mann-Whitney test; Figure 27). SLC40A1 expression appeared to be highest in healthy controls, lower in SHI[lo] COPD subjects, and the lowest in SHI[hi] COPD subjects, though there was no statistical difference between SHI[lo] and SHI[hi] (median 0.15[0.05,1.0] vs 0.18[0.06,0.28], p=0.86, Mann-Whitney test; Figure 28). There was no gene expression of TMPRSS6 in any of the samples.
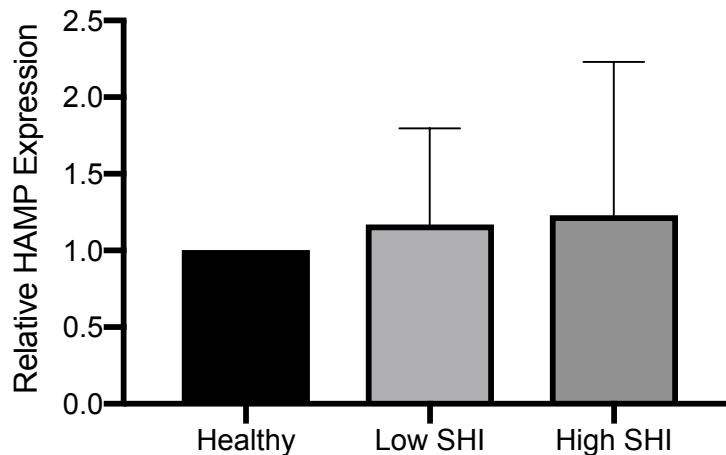
Figure 27: Relative expression of hepcidin gene in healthy controls and chronic obstructive pulmonary disease subjects with low and high sputum hemosiderin index. Data presented as mean±SD. HAMP, hepcidin anti-microbial peptide gene; SHI, sputum hemosiderin index.
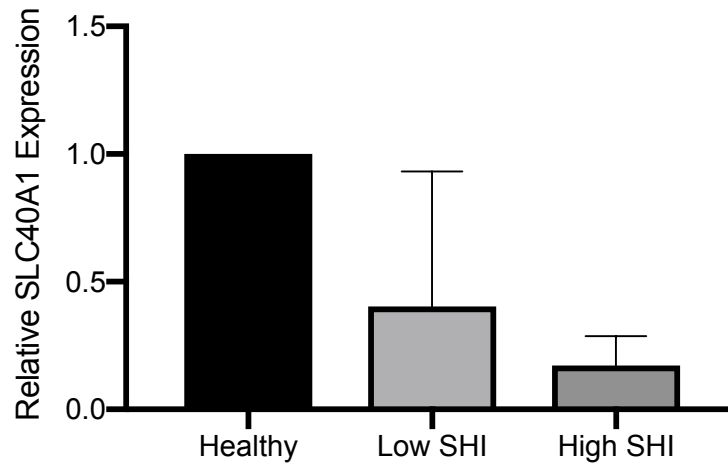
Figure 28: Relative expression of ferroportin gene in healthy controls and chronic obstructive pulmonary disease subjects with low and high sputum hemosiderin index. Data presented as mean±SD. SLC40A1, solute carrier family 40 member 1 gene; SHI, sputum hemosiderin index.

Discussion

In this chapter, in vitro macrophage models (cell-line or sputum cells) demonstrated that exogenous IL-6 or hepcidin, but not hi-HI, caused intracellular iron sequestration. This occurs even though hi-HI is associated with secretion of IL-6 and hepcidin from macrophages. The role of IL-6 but not hepcidin in iron sequestration is corroborated by patient data from a prospective COPD cohort, and this appears to be particularly true in the setting of TMPRSS6 genetic polymorphism.

Iron sequestration was measured either by measuring the iron directly in lysed cells with ICP-MS or by comparing the iron concentration in supernatant before and after treatment. The former showed significant sequestration with IL-6, hepcidin, and IL-6 and hepcidin together. The latter showed reduction in supernatant iron concentration

for IL-6, hepcidin, hi-HI, IL-6 and hi-HI, and hepcidin and hi-HI. Disagreement between these two measures could be explained by the release of intracellular elements with iron-binding capacity from hi-HI after lysis. The following discussion will consider the primary outcome of intracellular iron by ICP-MS as the more valid measure in cases of disagreement.

This study confirmed that IL-6 can cause iron sequestration within cell-line-derived macrophages in vitro, as proven by a reduction in the concentration of iron in the supernatant and subsequent increase in intracellular iron. The present model also confirmed that IL-6 release from macrophages is stimulated by the activation of PRRs (by hi-HI). Despite this, the presence of exogenous hi-HI in any of the conditions was sufficient to prevent iron sequestration. This could be related to the release of intracellular elements with iron-binding capacity. PRR activation by LPS has previously been shown to cause iron sequestration (46). The lack of significant iron sequestration in the combined IL-6 and hi-HI group suggests either that macrophage-derived IL-6 does not play a role in the release of hepcidin, perhaps related to overall low secreted quantities, or could be related to residual iron-binding capacity of the bacteria. Sputum macrophages isolated from healthy controls were also tested, and though the sample size was limited, these pulmonary macrophages trended towards behaving similarly in response to IL-6. From the prospective COPD cohort, there was a significant correlation between IL-6 and SHI, which suggests that IL-6 had the same effect in vivo. Finally, it

appears that in the presence of TMPRSS6 genetic polymorphism, high IL-6 drives the pulmonary sequestration of iron, much as it does systemically in anemia of chronic disease. However, if there is local action of matriptase-2, it is likely not occurring through airway leukocytes given the virtually non-existent expression of this gene in sputum cells.

Hepcidin was also confirmed to cause iron sequestration in vitro. Of the tested conditions, it was only released from macrophages in response to IL-6 with hi-HI, and not by IL-6 or hi-HI alone. A study of TDM had similar findings, as hepcidin was only induced by IL-6 when Mycobacterium avium was also present (40). Much like IL-6-treated cells, the addition of hi-HI appeared to prevent cellular iron sequestration. Hepcidin also appeared to contribute to iron sequestration within sputum macrophages. However, data from the prospective cohort did not support this finding, particularly as it pertains to macrophage-derived hepcidin. Firstly, there was no correlation between serum or sputum hepcidin and SHI. Secondly, despite a trend towards lower ferroportin gene expression in COPD subjects with high SHI relative to those with low SHI or healthy controls, the relative expression of HAMP was no different between these three groups.

This is the first study to examine the mechanisms of macrophage iron sequestration in human pulmonary macrophages. Although the sample size for SM experiments were

limited, in conjunction with the COPD cohort data, there appears to be evidence that

pulmonary macrophages behave differently than splenic macrophages in terms of iron

sequestration. The SM experiments potentially support the role of IL-6 and hepcidin

contributing to pulmonary iron sequestration, but the cohort data only found a

correlation between SHI and IL-6. Serum IL-6 and serum hepcidin are correlated, but

neither serum or sputum IL-6 were associated with sputum hepcidin for COPD patients.

Taken together, it appears that neither systemic or pulmonary IL-6 causes pulmonary

hepcidin secretion, and it is possible that IL-6 can cause iron sequestration through a

hepcidin-independent mechanism. Alternatively, the association between IL-6 and

raised SHI from the cohort data could be an epiphenomenon, with IL-6 increasing in

parallel with a true stimulus for sequestration, such as LPS (as demonstrated in [35]) in

the setting of infection.

The findings of this chapter provide conflicting evidence regarding the role of hepcidin

in pulmonary iron sequestration. While hepcidin appeared to reduce supernatant iron in

in vitro experiments, this was not supported by the prospective cohort data. The RT-

qPCR data also suggests that reduced ferroportin gene expression is important in

pulmonary iron sequestration, but that the role of macrophage-derived hepcidin is

either not important or redundant. Disagreement between in vitro and cohort data

could be related to differences in airway iron-binding capacity between healthy controls

and subjects with COPD. Mucin is one such protein that is present in higher

concentration in the airways of patients with chronic bronchitis, which can potentially

bind free iron (50,51). The difference between in vitro and cohort data was initially

considered to be related to the supra-physiologic concentration of hepcidin used in

experiments, but the only other study of human pulmonary macrophages found that a

similar concentration of hepcidin did not lead to increased intracellular iron in AMs (48).

This could be explained by inherent differences between AMs and SMs, with the latter

representative of the proximal rather than distal airways, or potentially related to the

higher yield of macrophages in AM experiments. The role of hepcidin in iron

sequestration is supported by a study of murine AMs which demonstrated that hepcidin

treatment led to downregulation of ferroportin (35). In splenic macrophages, iron

sequestration with IL-6 is considered to occur through hepcidin, but our findings

suggest IL-6 in the lungs could lead to iron sequestration independent of hepcidin.

Though it is plausible that IL-6 is elevated in situations where PRRs are also activated,

the present study found that hi-HI paradoxically attenuated iron sequestration. While

one previous study found that LPS caused iron sequestration (35), an IL-6-mediated but

hepcidin-independent mechanism is still possible. IL-6 and SHI have been correlated

previously in a study of COPD patients (36).

Limitations within this chapter include the small sample size of SMs, which limits the

strength of conclusions that can be drawn from these experiments. However, this data

was coupled with data from a large COPD cohort, which together presented a

convergent framework of pulmonary iron sequestration. Also, the relatively low yield of SMs prevented the measurement of intracellular ion, limited the number of conditions tested, and did not allow for the accurate measurement of macrophage-derived cytokines/proteins. In addition, RT-qPCR was only performed on sputum cell pellets from eight COPD subjects. Further research is required, with confirmation of the RT-qPCR data as well as experiments with alveolar macrophages obtained via bronchoscopy and bronchoalveolar lavage to improve yield.

The clinical applications of these findings are currently limited, but could be of importance if future research demonstrates that reducing pulmonary iron content could lead to benefit. This treatment strategy has been considered for cystic fibrosis (52) and pulmonary iron overload secondary to β-thalessemia, with evidence of reduced inflammation and generation of ROS in the latter condition (53). If non-chelator therapies to reduce pulmonary macrophage iron are considered in the future related to potential toxicity, targeting IL-6 may be more fruitful than targeting hepcidin.

Conclusion

The findings from this chapter re-confirmed the mechanisms linking systemic chronic inflammation and iron-overload through the hepcidin-ferroportin axis. More importantly, this chapter used human pulmonary macrophage experiments and a cohort of COPD patients to show that the role of hepcidin in pulmonary iron

sequestration is uncertain, but that IL-6 likely could lead to this phenomenon by an as-

yet undescribed hepcidin-independent mechanism.

Chapter 4: Does macrophage iron content increase the susceptibility to infection?

Background

Evidence Supporting Iron and Increased Susceptibility to Infection

The evidence supporting the concept of iron-overload predisposing to infection initially came from patients with conditions associated with iron overload (including β-thalassemia and hemochromatosis), with macrophage dysfunction being implicated as the mechanism. The immune functions of macrophages are multiple and include phagocytosis, cytokine release, efferocytosis, and the production of reactive oxygen species. Peripheral blood mononuclear cell (PBMC)-derived macrophages from patients with these iron-overload conditions have reduced phagocytic and bactericidal capacities, inhibited interferon-mediated activation, and reduced release of tumour necrosis factor-α (54,55).

There is also supportive experimental evidence implicating the macrophage, with chronic iron exposure shown to reduce bactericidal capacity (of *Escherichia coli* and *Pseudomonas aeruginosa*) in cell-line models, potentially related to the impairment of lysosomal acidification. These authors also demonstrated that bactericidal capacity was restored with a chelator (21). Similarly, iron-overload of murine cell-line macrophages (RAW264.7 cells) reduced the generation of reactive oxygen species. This study also found that experimentally infected mice with pharmacologic blockade of hepcidin had reduced cytosolic iron, and increased ROS generation, which was associated with reduced growth of *Salmonella* (47). Finally, murine macrophages treated with

exogenous hepcidin demonstrated increased growth of intracellular organisms,

including *Legionella* and *Chlamydia* (56).

Increased rates of infection are also posited to occur secondary to bacteria's increased

access to this essential nutrient. This is seen clinically where caution is exercised when

using iron infusions in the setting of possible infection, though the available population

data is conflicting in regards to this association (57,58). Experimental data is limited, but

has not demonstrated any differences in the growth of *Salmonella* when grown in

media containing increasing iron concentrations (47).

<u>Macrophage Dysfunction in COPD</u>

Macrophages from COPD patients (both PBMC-derived and alveolar) have been

extensively studied with respect to their anti-bacterial function. Reduced phagocytosis

of bacteria was seen in AM for non-typeable *Haemophilus influenzae* (NTHI) (59) and

Moraxella catarrhalis (MC) (60), with conflicting findings for *Streptococcus pneumoniae*

(SP) (60,61). Although there is evidence for impaired phagocytosis in AMs from COPD

patients, there appears to be no difference in bactericidal ability (59). Interestingly,

these studies did not demonstrate impaired function in monocyte-derived

macrophages from COPD patients, indicating a compartmental effect.

In addition, AMs from exacerbation-prone patients demonstrate reduced cytokine

release, including Interluekin-8 and tumour necrosis factor-α, in response to bacteria

and Toll-like Receptor (TLR) ligands (26). While the dysfunction of pulmonary macrophages from COPD patients is evident, the mechanism by which this occurs is unclear, and though iron content was not measured in these studies, it could potentially contribute.

A single study provides evidence that iron could contribute to pulmonary macrophage dysfunction. This ex vivo study demonstrated that murine AMs and cell-line derived macrophages loaded with an ambient particulate matter mix, including iron and other elements, reduced killing of SP secondary to an impairment in phagocytosis. Furthermore, phagocytic function was restored with a chelator, and then subsequently impaired again by the addition of exogenous iron (11).

There are multiple proposed mechanisms by which excess iron levels could contribute to increased bacterial infection, including impaired macrophage immune function, increased access to essential nutrients by bacteria, and even macrophage cell-death (by ferroptosis) leading to the release of pathogens (15,16,21). Given that pulmonary macrophages in COPD have dysfunction of unknown etiology and house the majority of iron within the lung, this thesis chose to focus on macrophage-related mechanisms of susceptibility to infection.

<u>Clinically Relevant Bacteria in COPD</u>

Culture and molecular sequencing studies have demonstrated that the most clinically relevant bacteria in COPD include *Haemophilus influenza* (HI), *Streptococcus pneumoniae* (SP), *Moraxella catarrhalis*, and *Pseudomonas aeruginosa*. These organisms are important as causes of acute exacerbation (AECOPD), with some contributing to inflammation in the setting of colonisation (62,63). To understand the role of excess iron on infective COPD exacerbations, it is important to examine disease-relevant organisms given that bacterial diversity is accompanied by differences in iron scavenging, the form of iron utilised by the organism, propensity for colonisation, and the interaction with human cells (26). Previous ex vivo macrophage studies have relied on cell-lines from mice or humans, and did not specifically examine iron-overload of specific compartments or account for specific respiratory infection-causing bacterial species. Although studies that established AM dysfunction in COPD did use clinically important bacteria, they did not attempt to identify the underlying cause of macrophage dysfunction.

This thesis sought to examine the effect of iron-overload on macrophage function using bacterial species which are clinically relevant to COPD with both cell-line-derived macrophages, and sputum macrophages isolated from COPD patients.

Methods

Bacterial Samples

Haemophilus influenzae and *Streptococcus pneumoniae* were chosen *a priori* for
experiments as they are two common causes of gram-negative and gram-positive
infectious AECOPD, respectively (64,65). The HI strains (P71B10 and P5602) were
clinical samples obtained frozen in glycerol from Dr. Michael Surette's laboratory, with
P71B10 isolated from one of the study patient's sputum by extended culture, and the
other being from an asthmatic. The SP strains (P1121 and P2140) were isolated from
nasopharyngeal samples and were obtained from Dr. Dawn Bowdish's laboratory frozen
in glycerol. Bacterial genus and species of all strains were confirmed by 16S rRNA
Sanger sequencing.

Bacteria Preparation

HI strains were streaked onto chocolate agar plates from a sample frozen with glycerol
the day prior to experiments. On the day of experimentation, 4-5 individual colonies
were transferred to Bacto™ Todd-Hewitt broth (THY; Becton, Dickinson and
Company™, Franklin Lakes, NJ) supplemented with 2% yeast extract (ThermoFisher
Scientific™, Waltham, MA) and incubated (at 37ºC and 5% CO_2) until an optical density
at 600 nm (OD_{600}) of 0.5 was reached. The SP strains were grown in broth from
previously prepared aliquots. These aliquots had been grown to an OD_{600} of 0.5 and
stored in 1mL aliquots with glycerol (10%) in Bacto™ tryptic soy broth (TSB; Becton,

Dickinson and Company™, Franklin Lakes, NJ) at -80ºC. This required initial streaking onto sheep's blood agar plates, and growth of 4-5 isolated colonies in TSB. On the day of experiments, an aliquot was thawed at room temperature and then added to 4mL of TSB and incubated (at 37ºC and 5% CO_2) until an OD_{600} of 0.5 was reached.

For both bacterial species, after the desired OD_{600} was achieved, 1mL of inoculated broth was centrifuged at 13500rpm for 1 minute and then resuspended in 1mL of sterile 1x Hank's balanced salt solution (HBSS) and rested on ice until the bacterial assays were to begin. Prior to this, bacterial titres were established by plating serial dilutions (10^{-1} to 10^{-7}) on the appropriate agar plate.

THP-1-Derived Macrophage Preparation

THP-1 cells were differentiated into TDMs (with PMA as previously described) in 10cm cell-culture treated dishes. After 48 hours, the media was aspirated and replaced with either control media (RPMI 1640 with L-glutamine [2mM], 10% fetal calf serum and PMA of 100nM) or iron-enriched media (supplemented with $FeSO_4$ at 250µM) for an additional 48 hours. Cells were harvested by aspirating the non-adherent cells, washing with 1x PBS, and detaching the adherent cells by incubating (37ºC and 5% CO_2) with 0.25% trypsin (Gibco™, Gaithersburg, MD) for 5 minutes and by applying a cell-scraper. Cell viability was confirmed by staining with 0.4% Trypan Blue (Gibco™, Gaithersburg, MD).

Bacterial Uptake and Killing Assays (TDM)

Viable TDMs (1×10^6 cells in 900µL) with or without iron-loading were combined with bacteria (1×10^7 cells in 100µL) in a 1.5mL tube to achieve a multiplicity of infection of 10 and incubated ($37°C$ and 5% CO_2) on a shaker at 200rpm. At 1-hour, 1.5-hours, 2-hours, 3-hours, and 5-hours, a 100µL aliquot was removed, centrifuged at 3000rpm for 4.5 minutes and then resuspended with 100µL of sterile 1x HBSS to remove extracellular bacteria. This solution was then serially diluted with sterile deionized water (10^{-1} to 10^{-5}) to lyse the macrophages, and then 10µL plated in duplicate on the appropriate agar. Agar plates were left under the hood to dry (approximately 10 minutes), and then incubated at $37°C$ and 5% CO_2 overnight. The next day, colony-forming units (CFU) were counted after 24-hours of incubation for each dilution where possible and CFU/mL calculated. The primary outcome of this experiment was the bacterial uptake of iron-loaded TDM, which was determined by comparing the CFU/mL to the control TDM at the 1-hour time point. Bacterial killing under each condition, a secondary outcome, was determined by comparing the CFU/mL at each time point with CFU/mL at 1-hour.

Sputum Macrophage Preparation

Sputum macrophages were isolated by plastic adherence from fresh sputum cell pellets (as described above) under one of two conditions: control media or media with 100nM of Deferoxamine (Abcam™, Cambridge, UK). These macrophages were obtained from

study patients during a period of clinical stability. The purity of macrophages was

confirmed by preparing a cytospin slide with H&E staining.

Bacterial Uptake and Killing Assays (Sputum Macrophages)

Viable sputum macrophages from the above two conditions were diluted to a

concentration of $6x10^4$ cells/mL with 1x HBSS and combined with P71B10 in a 1.5mL

tube to achieve a multiplicity of infection of 10 and then incubated (37^oC and 5% CO_2)

on a shaker at 200rpm. This strain of HI was chosen given that it was specific to COPD

(isolated from a study patient). The methods then proceeded as described above for

TDM with aliquots only removed at 1-hour and 1.5-hours due to the lower number of

cells available. Bacterial killing after 1.5-hour incubation was the primary outcome of

this experiment and was determined by comparing the CFU/mL at this time point with

the CFU/mL at 1-hour. The effect of chelation on bacterial uptake was determined by

comparing the CFU/mL between the two conditions at the 1-hour time point.

Statistics

Bacterial uptake and killing/growth were compared by Wilcoxon matched-pairs signed

rank test. Comparisons between two groups were tested by unpaired t-test (single time

point) or a mixed-effects model (at multiple time points). Linear regression and

Spearman correlation were used to determine the associations between SHI and

bacterial uptake in SM samples.

Results

<u>TDM Experiments</u>

For the *Haemophilus influenzae* strains, the iron-loaded cells demonstrated a 29%

reduction in bacterial uptake compared to the untreated cells (median 71 [62,85] %,

p=0.03, Wilcoxon matched-pairs signed rank test; Figure 29). Bacterial growth was

measured for further time-points for P71B10, which demonstrated that this strain

continued to grow despite the presence of TDMs. A mixed-effects model demonstrated

that the bacterial growth rate did not differ in iron-loaded cells compared to untreated

cells (Figure 30).
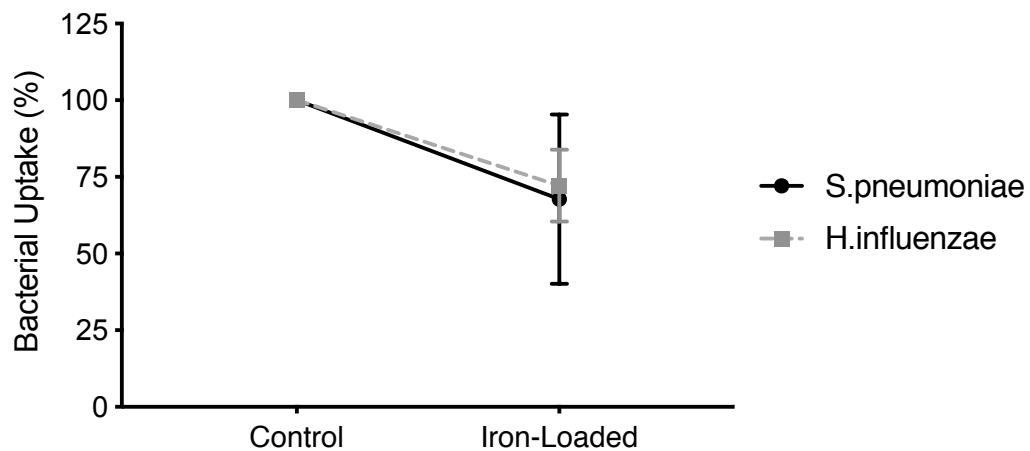
Figure 29: Percent uptake of Streptococcus pneumoniae and Haemophilus influenzae in iron-loaded and control THP-1-derived macrophages. Experiments performed in duplicate (n=6).
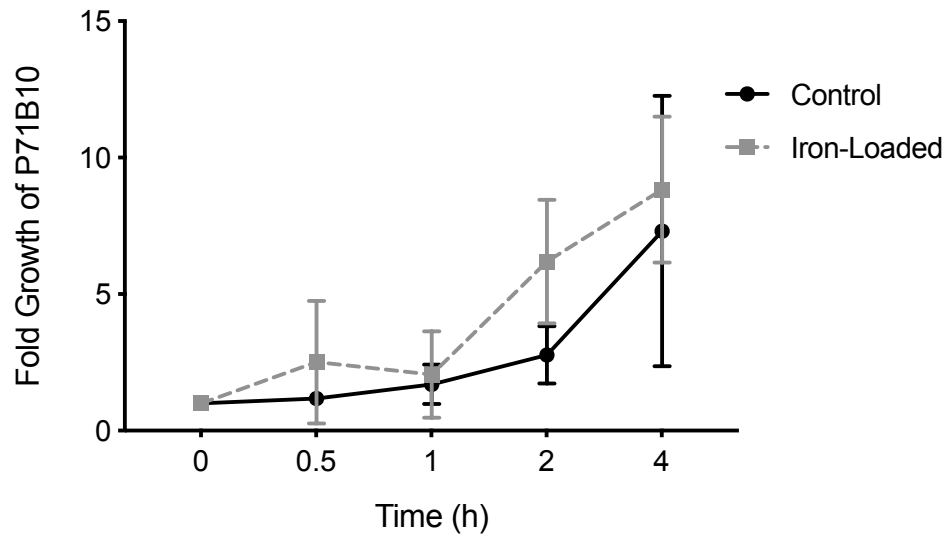
Figure 30: Fold growth rates of P71B10 strain of Haemophilus influenza in control and iron-loaded THP-1-derived macrophages over time. Experiments performed in duplicate (n=3).

For *Streptococcus pneumoniae* strains, the iron-loaded cells demonstrated 32% lower bacterial uptake compared to the untreated cells (median 68 [49,88] %, p=0.006, Wilcoxon matched-pairs signed rank test; Figure 28). Bacterial growth was measured for further time-points for P1121, which demonstrated that the growth of this strain was attenuated by TDMs. A mixed-effects model demonstrated that the bacterial growth rate did not differ in iron-loaded cells compared to untreated cells (Figure 31).
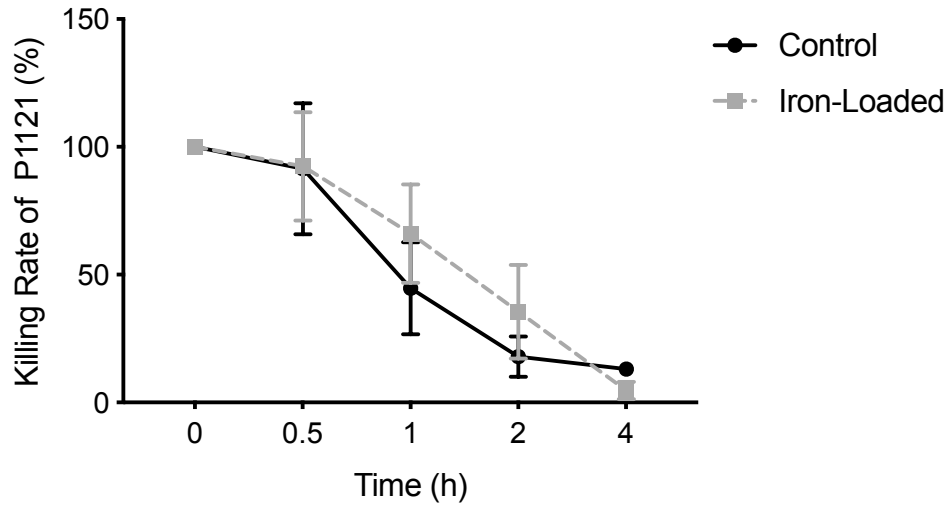
Figure 31: Bacterial killing of P1121 strain of Streptococus pneumoniae in control and iron-loaded THP-1-derived macrophages over time. Experiments performed in duplicate (n=3).

Sputum Macrophage Experiments

Ten subjects from the COPD cohort had their sputum macrophages isolated during a period of clinical stability. Among these ten, four were current smokers. Sputum macrophage purity was confirmed by H&E staining to be >85% for all samples, and overall viability by 0.4% Trypan Blue (Gibco™, Gaithersburg, MD) was 57±18%. There was no macroscopic evidence of contamination from non-experimental bacteria.

There was a trend towards correlation between sputum hemosiderin index and the bacterial killing rate at 0.5h (r=0.60, p=0.07, Spearman correlation), with linear regression shown in Figure 32. When these subjects were stratified into high and low SHI groups (≥20% vs 20%), there was also a near-significant difference in growth-rate (430±410% vs 170±24%, p=0.08, unpaired t-test, Figure 33).
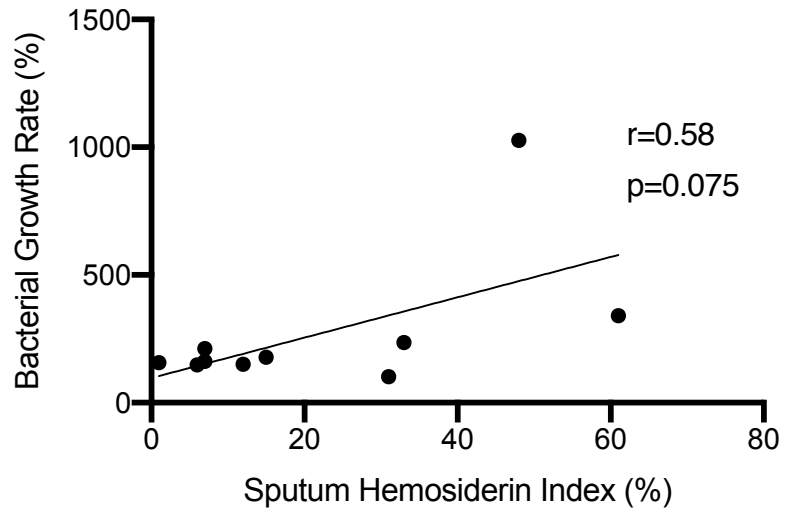
Figure 32: Linear regression of sputum hemosiderin index and growth rate of P71B10 after 90 minutes of incubation in sputum macrophages isolated from patients with chronic obstructive pulmonary disease.
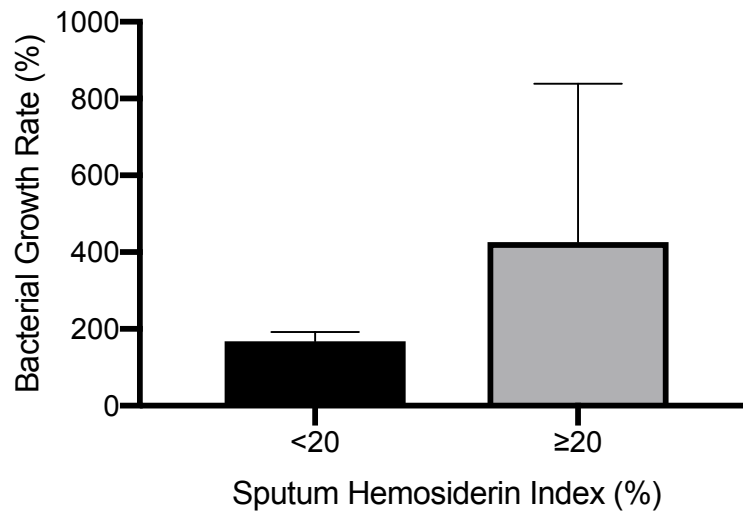
Figure 33: Bacterial growth rate of P71B10 after 90 minutes of incubation stratified by sputum hemosiderin index groups in patients with chronic obstructive pulmonary disease. Data presented as mean±SD.

Only three subjects had adequate sputum cell counts for experiments including

chelation. The sample size limited robust statistical analysis, but there appeared to be a

reduction in bacterial uptake with those sputum macrophages isolated with

Deferoxamine (Abcam™, Cambridge, UK) compared to untreated cells (Figure 34).
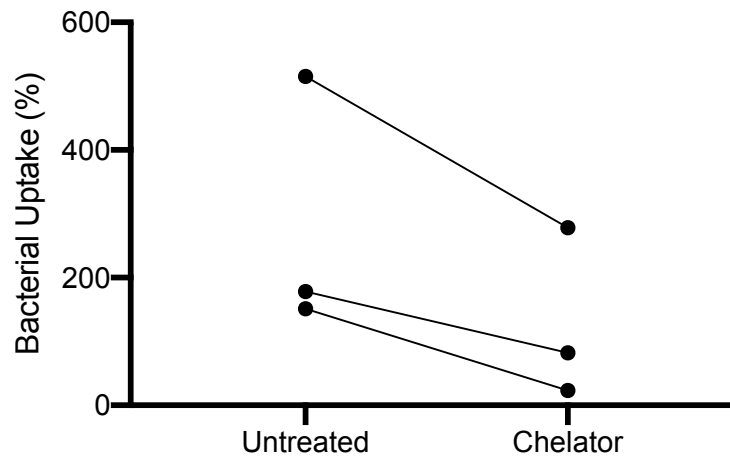
Figure 34: Bacterial uptake of P71B10 in untreated and chelator-treated sputum macrophages in patients with chronic obstructive pulmonary disease.

Discussion

In this chapter, iron-loading increased susceptibility to two bacterial species clinically

relevant to COPD in TDMs via reduction of bacterial uptake. On the other hand, in SMs

from COPD patients, there was supportive evidence that macrophage iron content was

associated with reduced bacterial uptake and killing rates of *Haemophilus influenzae*.

While for cell-line-derived macrophages the increased susceptibility to infection

appears to be driven by an impairment in phagocytosis, in SM, there may be an

additional impairment in bactericidal capacity. If this is a true difference, it would likely

be related to the conditioning occurring in vitro related to the microenvironment of the

COPD respiratory tract. These were not explicitly tested but could include macrophage polarization and other changes related to exposure to luminal cytokines, chemokines, danger-associated molecular patterns or pathogen-associated molecular patterns. This is the first study to assess the effect of iron content on human pulmonary macrophage immune dysfunction. Furthermore, organisms clinically relevant to COPD were tested, and SMs were isolated from patients with COPD and recent AECOPD, providing further specificity to the findings.

There are two previous studies examining iron-overload in macrophage models which have implicated an impairment in the intracellular killing rate. The first study saw that iron-loading did not change phagocytosis rates of *Escherichia coli*, but did cause a ~25% reduction in bacterial killing rate at four hours, which was reversed with a chelator (21). The second study tested murine cell-line macrophages and *Salmonella typhimurium*, and found reduced generation of ROS, but did not quantify bactericidal capacity in vitro in a macrophage model. Rather, these authors demonstrated that pharmacologic blockade of hepcidin in mice infected with *Salmonella* led to splenic macrophages with increased generation of ROS, which ultimately led to ~50% less growth of Salmonella and reduced mortality (47). The differences in findings between these studies and the current thesis could be secondary to a difference in the bacteria tested, bacterial assay used, or origin of the macrophages tested. Though *Escherichia coli* and HI are both gram-negative organisms, HI can cause intracellular infection particularly in the respiratory tract (66). In this study, HI in bacterial assays continued to grow, while SP

was controlled by macrophages, likely related to intracellular infection from HI. The phagocytosis assay used by Kao et al. measured fluorescently tagged bacteria (21), while this thesis used an uptake assay where CFU/mL were quantified. A strength of this thesis is the use of both human cell-line-derived macrophages and human sputum macrophages, and bacteria that are clinically relevant to COPD.

There are potential limitations to the experiments within this chapter. SM experiments were performed with a lower starting cell concentration due to the yield of cells often being low and dependent on samples obtained from subjects. However, this was accounted for by maintaining the same relative proportion of bacteria to macrophages (i.e. multiplicity of infection). The population of SMs isolated also likely had macrophage differences (e.g. maturity, polarization) between subjects secondary to the conditioning factors within the respiratory tract, which were not measured. With the relatively small number of cells isolated and number of subjects, it would have been difficult to completely characterise these cells and still perform the bacterial assays. However, one could argue for the importance of iron given that a near-significant association was seen based on this single factor.

Given these potential limitations and the in vitro nature of these experiments, an immediate clinical application of these findings is restricted. However, the results and their specificity to COPD will aid in building a foundation for further research, which

could eventually lead to novel therapies such as chelation. Inhaled chelators have been tested in animal-models and have been considered as a treatment in cystic fibrosis (52). Parenteral administration of chelators have been used in iron-overload mouse models and were effective at reducing the hemosiderin index of AMs (53). Finally, re-emphasizing currently used management strategies, including the optimisation of comorbid congestive heart failure, and smoking cessation, that also target known sources of pulmonary iron, could also be of additional benefit. Future directions include increasing the number of experiments performed for pulmonary macrophages from COPD patients, potentially using alveolar macrophages collected by bronchoscopy and bronchoalveolar lavage to improve total cell yield.

Conclusion

The main findings of this chapter demonstrate there could be differences in immune behaviour based on physiologic compartment, and provide in vitro evidence implicating excess iron as an infection susceptibility factor specific for COPD patients. Due to the limited sample size in SM experiments, further research with testing of human pulmonary macrophages and bacteria relevant to COPD is required to confirm this finding.

Chapter 5: Does sputum iron content predict infective exacerbations of COPD?

Background

As discussed in Chapter 1, COPD is associated with significant morbidity and mortality, and presents a significant burden in terms of healthcare utilisation. AECOPD are exceedingly common, yet attempts to risk stratify individuals is limited. The ECLIPSE cohort identified a history of previous exacerbation and FEV_1 as two of the only predictors of exacerbation (67). This can be partially attributed to the increasingly recognized disease heterogeneity that exists within COPD (68,69). The underlying etiology of an AECOPD can be variable and multiple, including incident infectious or eosinophilic airway disease, or worsening of airflow obstruction or hypercapnic respiratory failure (70). Therefore, considering AECOPD as a single and homogenous entity could obscure valid predictors of exacerbation of a specific etiology. To improve risk stratification strategies in COPD, we need inexpensive and clinically available tests driven by our understanding of pathophysiology, which can be applied to a targeted subset of AECOPD. SHI could potentially meet these criteria and requires further investigation.

<u>Measures of Iron</u>

Different strategies and methods have been utilised to non-invasively measure pulmonary iron. These studies typically examined in vitro mechanisms of iron sequestration (32), the relationship between airway iron and inflammation (71), or iron as a biomarker for pulmonary exacerbation (36,38). Measuring the cellular iron within

pulmonary macrophages has been commonly used, either by hemosiderin staining

(36,72) or by mass spectrometry or colorimetry after cell lysis (32,48). Alternatively, the

iron concentration of luminal secretions has been measured in the sputum supernatant

or bronchoalveolar lavage fluid (BALF) in studies involving induced sputum and

bronchoscopy, respectively. Less commonly, indirect strategies including the

measurement of iron-binding proteins, including intracellular ferritin or extracellular

transferrin, have been used (32).

<u>Clinical Studies Utilising Measures of Pulmonary Iron</u>

The diagnostic utility of hemosiderin index in alveolar macrophages was first tested in

an observational study of 101 patients who underwent bronchoscopy. Elevated

hemosiderin index was most prevalent in autoimmune-related alveolar hemorrhage,

post-transplant congestive heart failure, and infection (72). The use of this semi-

quantitative measure of iron in the sputum was further tested in patients considered to

be at risk for both cardiac and pulmonary causes of dyspnea, and found to be both

sensitive and specific for detecting cardiomyopathy (30).

Iron within the sputum supernatant has also been studied in the setting of inflammatory

airway diseases, mostly cystic fibrosis (CF), but also non-CF bronchiectasis, COPD and

asthma. In CF, due to the association of sputum iron with pro-inflammatory markers, it

was posited to be predictive of an impending infectious exacerbation (38). Another

study confirmed elevated sputum iron in CF, and also in non-CF bronchiectasis, where it

was negatively correlated with lung function, and positively correlated with

inflammatory cytokines or biomarkers, including Interleukin-8, calprotectin, and

myeloperoxidase (71). The amount of iron within whole sputum plugs of CF patients has

been measured in the setting of pulmonary exacerbation, only revealing a trend

towards lower iron levels after completing antibiotic treatment (73). These

observational studies predominantly examined a cohort of patients during exacerbation

and clinical stability, with minimal longitudinal data.

Studies of Pulmonary Iron In COPD

Sputum iron in COPD was first measured by authors interested in CF, to establish

baseline levels of iron in various respiratory conditions (38,71). Therefore, the clinical

impact of sputum iron was only examined for patients with CF and not COPD. Both of

these studies measured iron in the sputum supernatant, and while one study found

elevated iron in sputum supernatant compared to controls, the other did not (38,71).

The only COPD-specific study measured iron within sputum macrophages with the SHI

rather than in the supernatant (36). This study found that SHI measured at the time of

AECOPD strongly correlated with the number of infectious AECOPD that occurred in

the previous 1-year. Furthermore, it found an association between IL-6 and SHI, which

supported a potential mechanism of pulmonary macrophage iron sequestration.

Unfortunately, the outcome in this study was retrospective, and it could not objectively

confirm the presence or absence of an underlying infection as the cause for

exacerbation (36). To determine if the SHI is a valid predictor of infectious exacerbation,

this thesis pursued a prospective study of COPD patients with characterisation of

exacerbations as infectious or non-infectious.

Methods

<u>Patients</u>

Patients were recruited from a single-centre (St. Joseph's Healthcare Hamilton,

Charlton site) during an admission for AECOPD (listed as their primary diagnosis) from

December 2016 to May 2018. Inclusion in the study required age ≥40 years, and

incompletely reversible airflow obstruction (FEV_1/FVC<0.7) or radiologic evidence of

emphysema, in the setting of a ≥10 pack-year history of cigarette smoking. Those who

required admission to the intensive care unit, were unable to produce a spontaneous

sputum, or had a history of asthma or bronchiectasis of greater than mild severity

radiographically, were excluded. Fifty subjects were required to detect a hemosiderin-

attributed reduction in infective exacerbations of 30% using a multivariate regression

model (with 2 predictors) and a prediction level of τ=0.92.

After the initial exacerbation, patients entered a 1-year follow-up phase where they

were monitored for infectious exacerbations requiring admission to hospital (primary

outcome). The time to first infective exacerbation requiring admission to hospital was

used as a secondary outcome. At the time of AECOPD an underlying infectious etiology

was investigated by nasopharyngeal swab respiratory virus polymerase chain reaction

(NPS-PCR), sputum culture, and sputum differential and cell count (Figure 35).

Infectious exacerbation was defined as ≥1 of: positive respiratory virus NPS-PCR,

positive sputum culture, and/or total sputum neutrophil count ≥12 million cells/gram of

sputum. AECOPD was confirmed by study personnel by the presence of Anthonisen

criteria (either a change in sputum appearance or volume, or increased dyspnea).
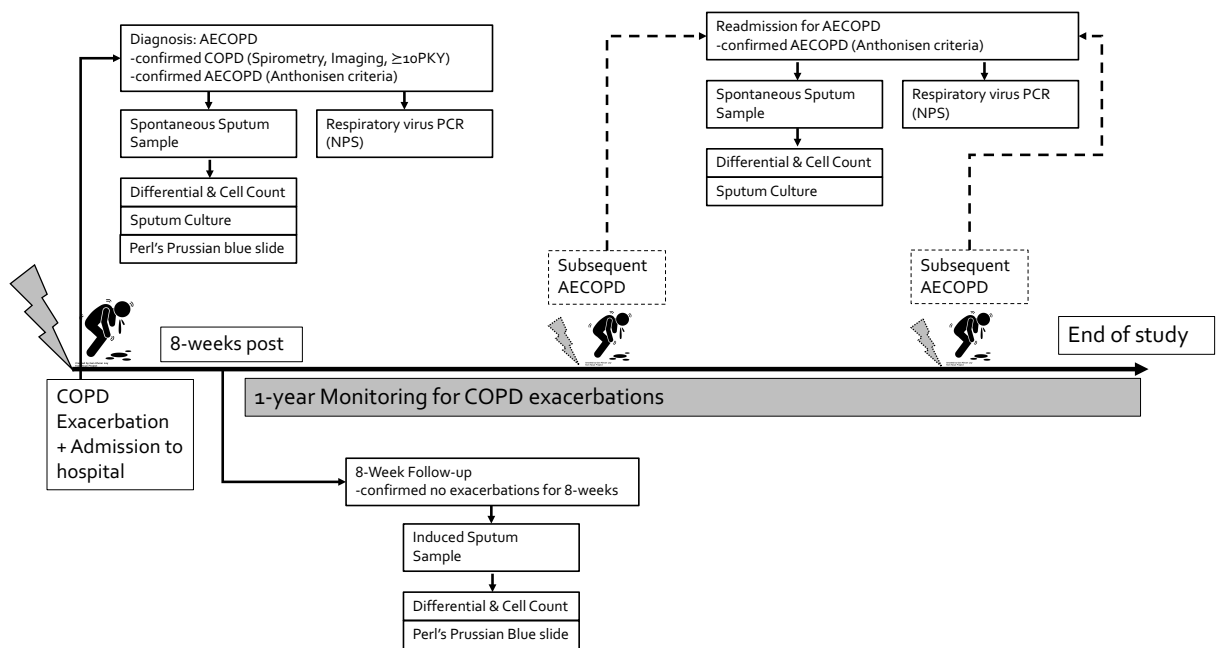
Figure 35: Objective 3 study design. AECOPD, acute exacerbation of chronic obstructive pulmonary disease; COPD, chronic obstructive pulmonary disease; PKY, pack-years; PCR, polymerase chain reaction; NPS, nasopharyngeal swab.

Baseline Characteristics and Clinical Testing

Clinical covariates including demographics, comorbid cardiac disease, smoking

history/status, vaccination history, exacerbation history, and COPD-related treatment

(pharmacologic and non-pharmacologic) were collected.

Routine testing as per best care practices was followed, including blood gases, NPS-

PCR, sputum cultures, and chest imaging. Systemic iron status was assessed directly

with serum ferritin, transferrin and iron, and indirectly with a complete blood count

(including hemoglobin and mean corpuscular volume).

Sputum Collection and Processing

At the time of enrollment and for all subsequent AECOPD, spontaneous sputum

samples were collected from patients. During clinical stability (at least 8 weeks from

their discharge from hospital), either spontaneous or saline-induced samples were

collected. Saline induction required serial inhalation of increasing concentrations of

saline. The starting concentration of saline was lower depending on the severity of FEV_1

impairment, as per local protocol. Samples underwent sputum plug selection by

inverted microscopy, mucous dispersion by dithiothreitol (DTT; Sigma-Aldrich™, St.

Louis, MO), and filtering with 53μm nylon mesh (as previously described in (74)). Cells

were counted in a hemocytometer and their viability assessed with 0.4% Trypan Blue

(Gibco™, Gaithersburg, MD) staining. The resulting filtrate was centrifuged to produce

cell-free supernatant and a cell pellet with storage at -80ºC.

Blood Collection

During initial AECOPD and during a period of clinical stability, blood was collected in

collection tubes with a clot activator and centrifuged to yield a serum sample, and

PAXGene™ tubes (PreAnalytix™) for storage of whole blood mRNA. Both sample types

were stored at -80°C.

Informed Consent and Ethics

Informed consent was obtained from all subjects. The study was approved by the

Hamilton Integrated Research Ethics Board.

Statistics

Descriptive statistics were used to summarise subject characteristics and exacerbation

data, with mean±SD for parametric data and median (IQR) for non-parametric data.

Measures of iron in the sputum at the time of exacerbation and while clinically stable

were compared with unpaired t-test (for parametric data) and Mann-Whitney test (for

non-parametric data).

To explore the association between SHI and exacerbation, linear regression between

SHI (at AECOPD or follow-up) and infective exacerbations was performed initially. Then

a negative binomial regression was utilised due to over-dispersion of the primary

outcome (infective exacerbations) with adjustment for FEV_1%Predicted and the number of admissions for AECOPD in the previous 1-year. Time-to-event analysis was performed for first infective exacerbation, with the difference between low and high SHI groups presented as a hazard ratio (HR). Significance between groups was tested with the Mantel-Haenszel test. Subjects were censored at death, study withdrawal, or if lost to follow-up.

Results

<u>Subjects</u>

Fifty-six subjects met the inclusion criteria and consented to participate in the study, of which 49 completed the 1-year monitoring period. Seven subjects were lost to follow-up due to death (n=4), being unreachable by telephone (n=2), and withdrawing due to a new diagnosis of cancer (n=1). The descriptive data described a study population which overall was Caucasian with severe COPD, of which approximately half were current smokers and one-third used supplemental oxygen. Echocardiograms were available in 40 subjects, which revealed 12 subjects with diastolic dysfunction alone, 3 subjects with systolic dysfunction (ejection fraction <55%) alone, 2 subject with systolic and diastolic dysfunction, and 1 subject with moderate aortic stenosis. Their demographics, baseline characteristics and relevant medications are summarised in Tables 2-3.

Demographics	Value
Number of Participants	49
Age (years)	67 ± 9
M/F	32/17
Caucasian (%)	94
COPD-Related Variable	
Current Smoker (%)	57.1
Smoking history (pack-years)	50 (39,63)
Radiographic Emphysema (%)	90.6
Home O_2 (%)	38.3
FEV_1 (L)	1.1 ± 0.47
FEV_1 (%Predicted)	41 ± 18
Self-reported AECOPD in last 1-year	2 (0,4)
Self-reported Admission for AECOPD in last 1-year	0 (0,1)

Table 2: Baseline demographics and variables related to chronic obstructive pulmonary disease of the prospective cohort. Data presented as mean±SD, proportions, or median (IQR). M/F, male/female; FEV_1, forced expiratory volume in 1 second; AECOPD, acute exacerbation of chronic obstructive pulmonary disease.

Medication Use	Frequency
LAMA	45 (91.8%)
Inhaled Corticosteroid	43 (87.5%)
LABA	40 (81.6%)
ACE inhibitor	20 (41.3%)
Loop diuretic	10 (20.8%)
Chronic Azithromycin	4 (8.5%)
Spironolactone	1 (2.0%)
Roflumilast	1 (2.0%)
Theophylline	0 (0%)

Table 3: Proportion of relevant medication use in the prospective cohort. LABA, long-acting beta agonist; LAMA, long-acting muscarinic antagonist; ACE, angiotensin converting enzyme.

Systemic Iron Status of Subjects

Systemic iron studies including serum ferritin, iron and transferrin, as well as

hemoglobin and mean cell volume at AECOPD and follow-up (disease quiescent period)

are summarised in Table 4.

Anemia Data	AECOPD	Follow-up
Hemoglobin (g/L)	135 ± 19.8	131 ± 16.4
Mean cell volume (fL)	93.4 (89.8, 97.2)	89.0 ± 10.5
Ferritin (μg/L)	127 (79.0, 309)	112 (31.0, 186)
Iron (μmol/L)	9.00 (6.00, 13.0)	12.0 (9.00, 15.0)
Transferrin (g/L)	2.18 (1.86, 2.61)	2.71 ± 0.511

Table 4: Systemic iron status of prospective cohort at AECOPD and follow-up. Data presented as mean±SD or median (IQR). AECOPD, acute exacerbation of chronic obstructive pulmonary disease.

Measurements made at the time of AECOPD revealed anemia (Hemoglobin <130 g/L) in

35% of subjects, with concurrent microcytosis (MCV <82 fl) in 17%. Clinical entities of

probable iron-deficiency (ferritin <23 µg/L) and possible iron-overload (ferritin >400

µg/L) were present in 19.5% and 14.6%, respectively. Iron levels were lower than the

lower limit of normal in most subjects (87.5%). A pattern in keeping with anemia of

chronic disease (microcytosis with reduced iron and elevated transferrin) was only seen

in 2.4%.

During follow-up, anemia was present in 43% of subjects, of which 14% were

microcytic. Probable iron-deficiency was present in 14.8% and possible iron-overload in

7.4%. Iron levels were lower than the lower limit of normal in 33.3%. Anemia of chronic disease was present in 7.4%.

Exacerbations & Readmissions

Amongst subjects' first admissions, 32 were secondary to infection while 17 were non-infectious (criteria as defined in Methods). In cases where an infective exacerbation was confirmed, it was done so by bacterial culture in 10 (31%), by NPS-PCR (without positive bacterial culture) in 10 (31%), and by differential and cell count alone in 12 (38%).

The bacteria isolated in culture and virus detected by NPS-PCR from all exacerbations are summarised in Figures 36-37. In addition, mycobacterial and fungal cultures of the sputum during exacerbation grew *Mycobacterium avium* complex and *Aspergillus* species on four occasions each, but these were not considered by the treating physicians to fulfill the criteria for infection.
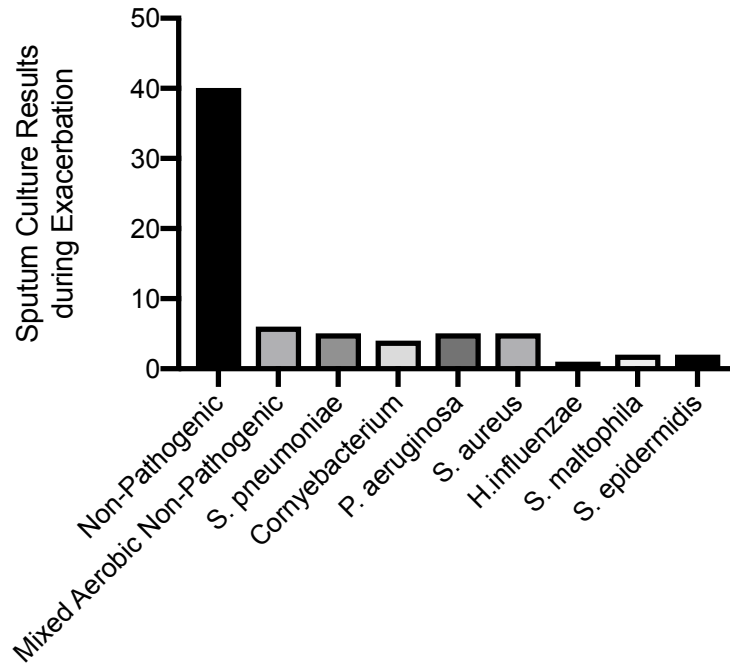
Figure 36: Bacteria grown on sputum culture at the time of exacerbation in prospective COPD cohort.
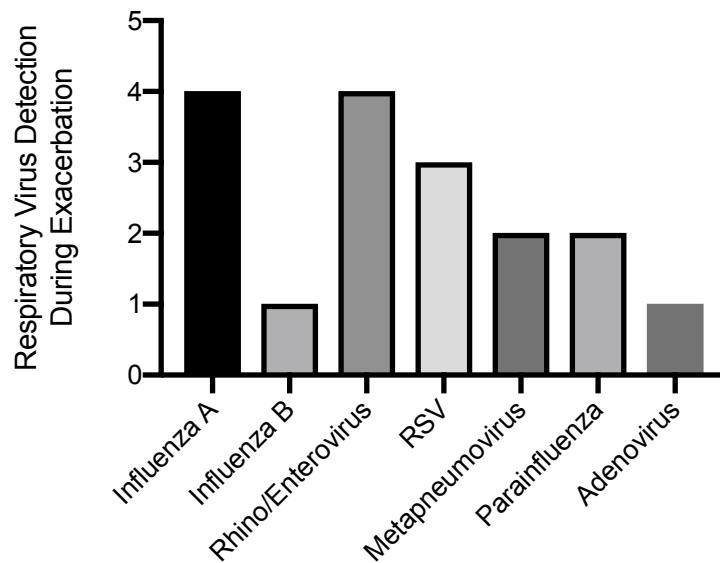
Figure 37: Respiratory viruses detected by nasopharyngeal swab polymerase chain reaction at the time of exacerbation in prospective COPD cohort. RSV, respiratory syncytial virus.

There were 73 readmissions for AECOPD during the monitoring period. Analysing by patient revealed that there was a median of 1(0,2), or mean of 1.49±1.56, readmissions (Figure 38). A corresponding sputum sample and viral NPS-PCR were collected in 40 (55%) and 52 (71.2%) of these episodes, respectively, of which 33 (45.2%) were proven to be infective exacerbations. In cases where an infective exacerbation was confirmed, it was done so by bacterial culture in 15 (45.5%), by NPS-PCR (without positive bacterial culture) in 5 (15.1%), and by differential and cell count alone in 13 (39.4%).
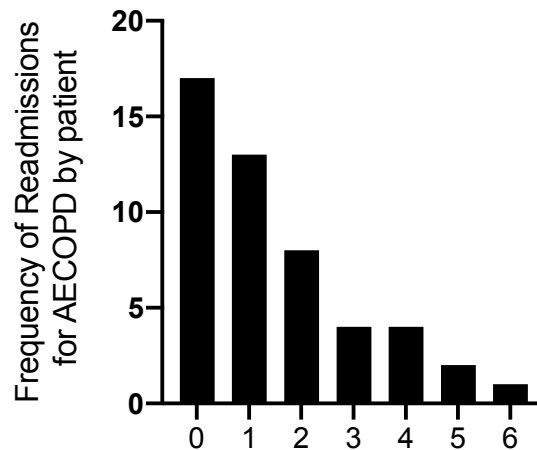
Figure 38: Histogram of the frequency of readmissions due to chronic obstructive pulmonary disease exacerbation in the prospective cohort. AECOPD, acute exacerbation of chronic obstructive pulmonary disease.

Sputum Hemosiderin Index at AECOPD and Follow-up

The sputum hemosiderin index collected during clinical stability was significantly higher than during AECOPD (median 2.5[1.0,8.8] vs 14[4.3,31], p=0.0001, Mann-Whitney test; Figure 39). The levels of unbound iron were also measured in the sputum supernatant

during clinical stability and AECOPD, demonstrating a reduction in iron concentration when clinical stability was achieved (2.6±0.73 vs 3.1±0.82 μM, p=0.015, unpaired t-test; Figure 40).
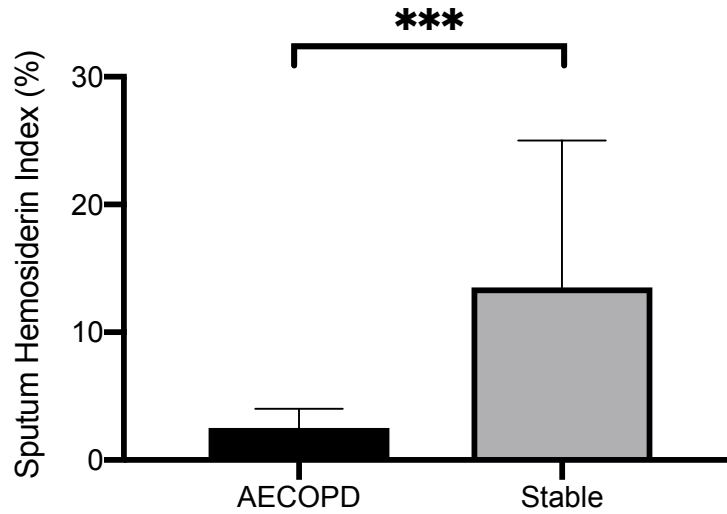
Figure 39: Sputum hemosiderin index in subjects during acute exacerbation and clinical stability. *** denotes p<0.001. AECOPD, acute exacerbation of chronic obstructive pulmonary disease.
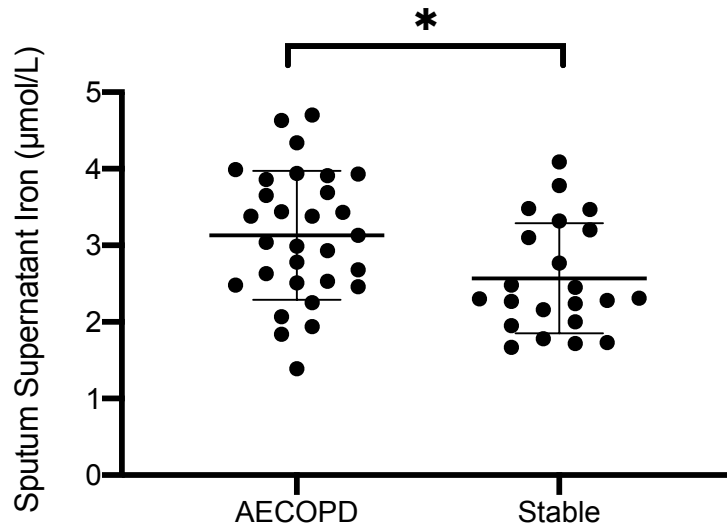
Figure 40: Sputum supernatant iron concentration in subjects during acute exacerbation and clinical stability. * denotes p<0.05. AECOPD, acute exacerbation of chronic obstructive pulmonary disease.

Linear regression of infective exacerbations and SHI at AECOPD and while clinically stable were not significant (Figures 41-42).
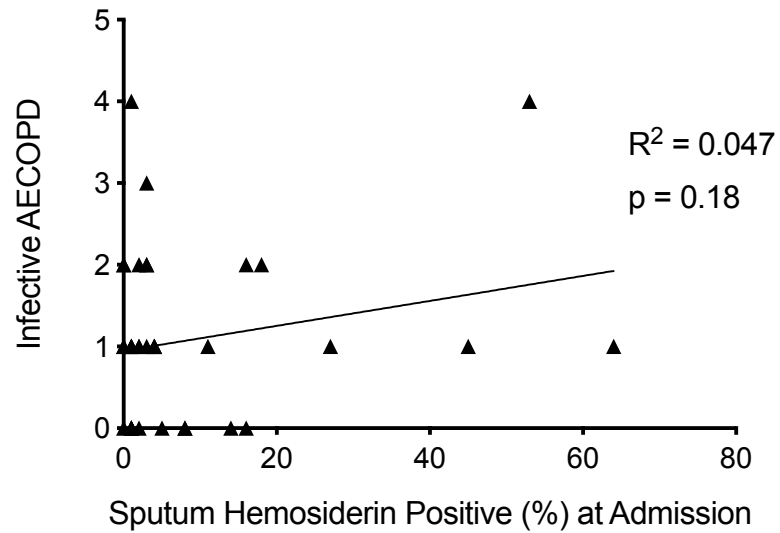
Figure 41: Linear regression of sputum hemosiderin index at admission and infective exacerbation of chronic obstructive pulmonary disease. AECOPD, acute exacerbation of chronic obstructive pulmonary disease.
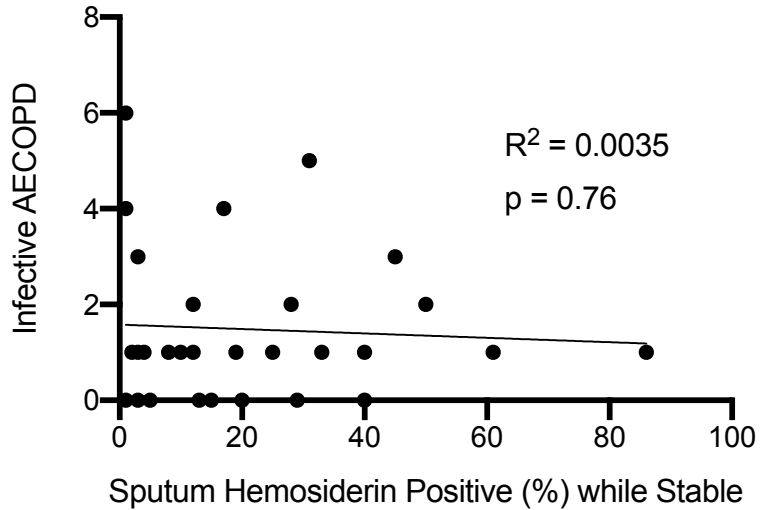
Figure 42: Linear regression of sputum hemosiderin index while clinically stable and infective exacerbation of chronic obstructive pulmonary disease. AECOPD, acute exacerbation of chronic obstructive pulmonary disease.

Negative binomial regression was performed for SHI at AECOPD and during a clinically stable period, accounting for covariates of FEV_1%Predicted and the number of admissions for AECOPD in the last 1-year. In the first model, SHI at AECOPD was not predictive of future infective exacerbation of COPD (beta-coefficient 0.012, p=0.5), while there was a trend for FEV_1%Predicted (beta-coefficient -0.043, p=0.057). The second model identified SHI (while clinically stable) as a near-significant predictor of infective exacerbations (β=0.035, p=0.051), while FEV_1%Predicted was significant (β=-0.051, p=0.017)

Time-to-first-infective-exacerbation analysis revealed no difference between those with SHI ≥10% and SHI <10% when measured during AECOPD (HR 1.67 95%CI: 0.51-5.4,

p=0.4, Mantel-Haenszel test; Figure 43) or during a period of clinical stability (HR 1.61

95%CI: 0.61-4.2, p=0.34, Mantel-Haenszel test; Figure 44).
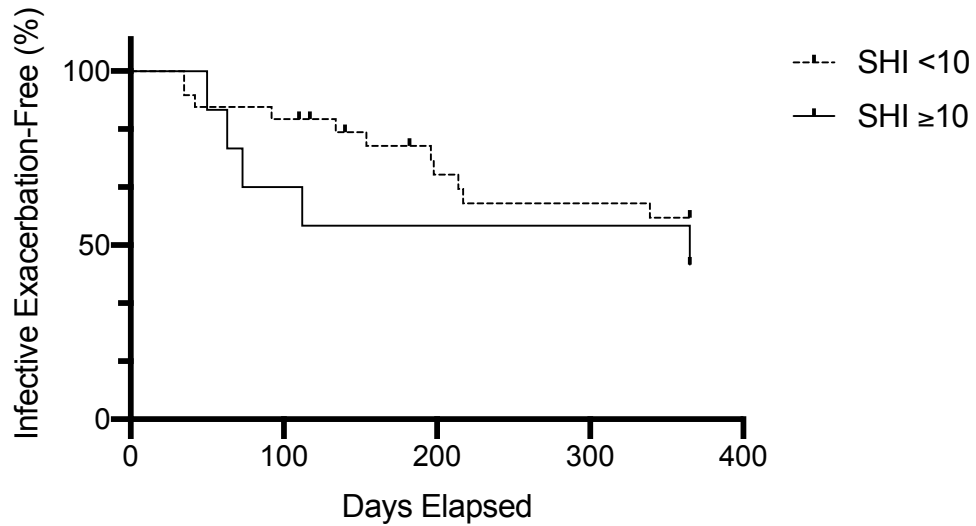
Figure 43: Kaplan-Meier curve demonstrating time to first infective exacerbation based on sputum hemosiderin index during exacerbation. SHI, sputum hemosiderin index.
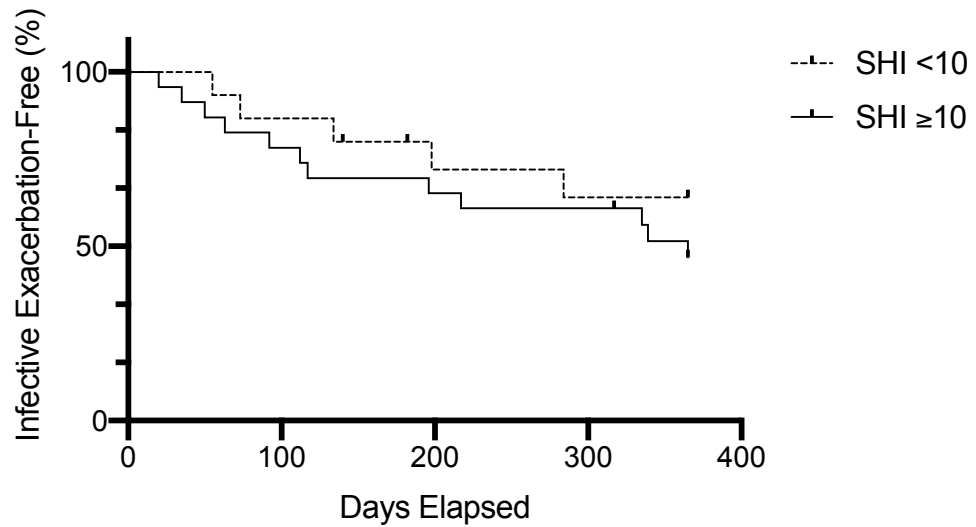
Figure 44: Kaplan-Meier curve demonstrating time to first infective exacerbation based on sputum hemosiderin index during clinical stability. SHI, sputum hemosiderin index.

Discussion

In this chapter, a prospective COPD cohort assessed predictors of proven infective exacerbations and found significance in support of FEV_1 %Predicted, and near-significance in support of iron content within sputum macrophages. There was no difference in time-to-first-infective exacerbation based on SHI.

Measures of systemic iron homeostasis in this population revealed a moderate to high proportion of abnormalities including anemia, iron-deficiency, possible iron-overload, and anemia of chronic disease, which are known to occur in COPD populations (13). Pulmonary macrophage iron varied between patients and with AECOPD. During AECOPD, free sputum iron increased, and after the exacerbation resolved, free sputum iron decreased with a concomitant increase in SHI, suggestive of active pulmonary macrophage iron sequestration. Considering the IL-6 data presented in the previous chapter, it is plausible that those individuals with an increase in IL-6 associated with AECOPD begins an iron sequestration process that ultimately leads to elevated SHI detected after the exacerbation event.

Linear regression and time-to-first-infective-exacerbation analysis suggested SHI was not predictive of infective exacerbations. However, given the over-dispersion of AECOPD, a negative binomial regression was used, and this analysis revealed that SHI

at the time of exacerbation is likely a predictor of infective exacerbations (which was

limited by the cohort sample size).

This is the second study which evaluates airway iron as a potential biomarker predictive

of AECOPD. The previous study showed that SHI had a higher beta-coefficient of 1.04 in

the prediction of infective AECOPD (36). This chapter used a prospective outcome with

a more robust definition of infective exacerbations, rather than relying on antibiotic use

and patient report, and is thus a more valid assessment of this biomarker.

There is a paucity of clinically available predictors of AECOPD. This chapter

demonstrates that SHI has the potential to risk stratify patients specifically for infective

exacerbation. Knowing that a specific patient is more prone to infective exacerbations

could facilitate individualized treatment. For healthcare providers faced with AECOPD,

this measure could influence the ordering of investigations (e.g. sputum culture or NPS-

PCR) and therapies such as antimicrobials. Action plans for outpatient AECOPD could

also be impacted, perhaps by starting with an antibiotic and then only progressing to

oral corticosteroids if there is no improvement. This could potentially reduce the

adverse-effects associated with repeated courses of corticosteroids.

Potential limitations include not accounting for AECOPD managed as an outpatient and

inpatient AECOPD where sputum was not collected. However, the nature of

exacerbations is difficult to characterise without thorough investigation which is at

times only possible while in hospital. Furthermore, this study captures severe

exacerbations, which is important given that these episodes contribute the most to

healthcare utilisation, and should be a priority to prevent. While only 55% of

exacerbations had a valid sputum result, many of these are likely related to a lack of

bronchitis.

Conclusion

This chapter provides evidence that AECOPD is associated with increased free iron in

the airways, which is subsequently sequestered in pulmonary macrophages (potentially

by IL-6). The resultant SHI is a promising biomarker for COPD, due to its predictable

increase after exacerbation, and its potential for predicting at risk of infective AECOPD.

Summary

In this thesis, experiments investigating the mechanisms of pulmonary iron sequestration and consequent macrophage dysfunction were paired with a prospective cohort study of COPD, to understand if there is a coherent pathophysiologic mechanism by which increased macrophage iron could predispose to infective AECOPD. Although further research is required due to limited sample sizes for some of the experiments, this thesis provides supportive evidence that excess airway macrophage iron can predispose patients with COPD to recurrent infective exacerbations.

Regarding the mechanisms of pulmonary iron sequestration, this thesis provides in vitro and population-level evidence that it is associated with IL-6, but could potentially occur independent of hepcidin. The role of hepcidin remains unclear, with disagreement between in vitro experiments and the prospective cohort, which could be potentially explained by differences in iron-binding capacity associated with disease (e.g. mucin concentration). RT-qPCR experiments of healthy controls and COPD patients were of limited sample size, but suggest that macrophage-derived hepcidin is either redundant or unimportant to pulmonary iron sequestration, but that ferroportin could play a role. There is still uncertainty regarding the roles of hepcidin and ferroportin in LPS and IL-6-mediated pulmonary iron sequestration, which could be addressed by siRNA experiments. Specifically, one could quantify iron sequestration in healthy SM after

exogenous LPS and IL-6 with or without experimental transfection with hepcidin-specific and IL-6-specific siRNAs. Furthermore, it is unclear if SM from healthy controls and COPD subjects behave differently, potentially related to airway iron-binding capacity or macrophage conditioning secondary to airway environmental stimuli. This could be addressed by performing exogenous IL-6 and hepcidin experiments with SM isolated from COPD subjects.

Experiments with TDM and SM from COPD subjects demonstrated that macrophage iron content could increase susceptibility to infection from bacteria that are relevant to COPD. In TDM, uptake of SP and HI were impaired in iron-loaded cells versus control. SM experiments suggested that iron content was associated with HI killing and uptake. Due to a limited sample size for SM experiments, there is still uncertainty regarding the effect of pulmonary macrophage iron content on susceptibility to infection, which could be addressed by performing more experiments.

Finally, the prospective cohort outlined the journey of airway iron in relation to AECOPD and provided data to support the increased propensity to infection seen in experimental models. It appears that free sputum becomes elevated at an exacerbation, as judged by significantly higher levels at AECOPD compared to follow-up. The reduction in free iron is accompanied by an increase in SHI at follow-up, suggesting that SMs are sequestering this iron. Excess iron in these SM measured at

follow-up was nearly predictive (p=0.051) of infective exacerbations in a negative

binomial regression model. While this association was seen in our previous published

manuscript, this thesis used a more robust definition of infective exacerbation. While

SHI is emerging as a promising biomarker to predict recurrent infectious AECOPD,

further prospective validation with a larger sample size is required to ultimately prove

its clinical utility.

The findings from each objective of this thesis provide important elements of a

theoretical model that links iron dysregulation and susceptibility to infection in COPD

(conceptual model shown in Figure 45). During an exacerbation, there is a release of

free iron into the airways, which can be accompanied by acute airway inflammation.

The exacerbation-associated increase in sputum IL-6 initiates a pathway by which

luminal macrophages start sequestering iron. As a patient recovers from their AECOPD,

free sputum iron is sequestered by pulmonary macrophages for the purposes of

nutritional immunity and to prevent excess formation of free oxygen radicals, but

ultimately this leads to immune dysfunction in these macrophages. In turn,

macrophage dysfunction will increase susceptibility to respiratory tract infection, which

can feedback into airway inflammation to create a cyclic pattern of infectious AECOPD.
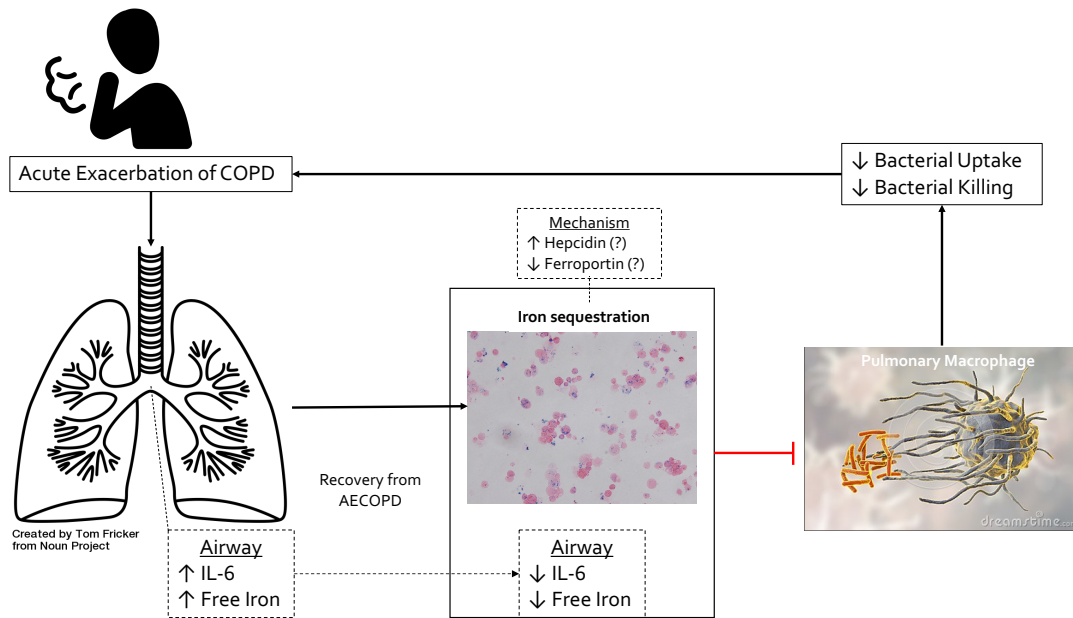
Figure 45: *Conceptual model of pulmonary iron dysregulation and recurrent infective exacerbations of chronic obstructive pulmonary disease. COPD, chronic obstructive pulmonary disease; IL-6, interleukin-6. Free images sourced from thenounproject.com and dreamstime.com.*

References

1.   O'Donnell DE, Aaron S, Bourbeau J, Hernandez P, Marciniuk DD, Balter M, et al. Canadian Thoracic Society recommendations for management of chronic obstructive pulmonary disease - 2007 update. Can Respir J. 2007;14 Suppl B:5B–32B.

2.   O'Donnell DE, Hernandez P, Kaplan A, Aaron SD, Bourbeau J, Marciniuk D, et al. Canadian Thoracic Society recommendations for management of chronic obstructive pulmonary disease - 2008 update - highlights for primary care. Can Respir J. 2008;15 Suppl A:1A–8A.

3.   Connors AF, Dawson NV, Thomas C, Harrell FE, Desbiens N, Fulkerson WJ, et al. Outcomes following acute exacerbation of severe chronic obstructive lung disease. Am J Respir Crit Care Med. 1996;154(4):959–67.

4.   Dickson RP, Martinez FJ, Huffnagle GB. The role of the microbiome in exacerbations of chronic lung diseases. Lancet. 2014;384(9944):691–702.

5.   Bloom D, Cafiero E, Abrahams-Gessel S, Jane-Llopis E, Bloom LR, Fathima S, et al. The global economic burden of non-communicable diseases: a report by the World Economic Forum and the Harvard School of Public Health. 2011. Geneva: World Economic Forum.

6.   Donaldson GC, Wedzicha JA. COPD exacerbations. Thorax. 2006;61(2):164–8.

7.   Pradan L, Ferreira I, Postolache P. The quality of medical care during an acute exacerbations of chronic obstructive pulmonary disease. Rev Med Chir Soc Med Nat Iasi. 2013;117(4):870–4.

8.   Seemungal TAR, Wilkinson TMA, Hurst JR, Perera WR, Sapsford RJ, Wedzicha JA. Long-term erythromycin therapy is associated with decreased chronic obstructive pulmonary disease exacerbations. Am J Respir Crit Care Med. 2008;178(11):1139–47.

9.   Martinez FJ, Calverley P, Goehring U-M, Brose M, Fabbri LM, Rabe KF. Effect of roflumilast on exacerbations in patients with severe chronic obstructive pulmonary disease uncontrolled by combination therapy (REACT): a multicentre randomised controlled trial. Lancet. 2015;385(9971):857–66.

10. Filho FSL, Ra SW, Mattman A, Schellenberg RS, Criner GJ, Woodruff PG, et al. Serum IgG subclass levels and risk of exacerbations and hospitalizations in patients with COPD. Respir Res; 2018;19:1–10.

11. Zhou H, Kobzik L. Effect of concentrated ambient particles on macrophage phagocytosis and killing of Streptococcus pneumoniae. Am J Respir Cell Mol Biol. 2007;36(4):460–5.

12. Reid DW, Anderson GJ, Lamont IL. Role of lung iron in determining the bacterial and host struggle in cystic fibrosis. Am J Physiol Lung Cell Mol Physiol. 2009;297(5):L795–L802.

13. Cloonan SM, Mumby S, Adcock IM, Choi AMK, Chung KF, Quinlan GJ. The "Iron-"y of iron overload and iron deficiency in chronic obstructive pulmonary disease. Am J Respir Crit Care Med. 2017;196(9):1103–12.

14. Nairz M, Schroll A, Demetz E, Tancevski I, Theurl I, Weiss G. "Ride on the ferrous wheel" – The cycle of iron in macrophages in health and disease. Immunobiology. 2015;220(2):280–94.

15. Amaral EP, Costa DL, Namasivayam S, Riteau N, Kamenyeva O, Mittereder L, et al. A major role for ferroptosis in Mycobacterium tuberculosis-induced cell death and tissue necrosis. J Exp Med. 2019;216(3):556–70.

16. Martins R, Maier J, Gorki A-D, Huber KVM, Sharif O, Starkl P, et al. Heme drives hemolysis-induced susceptibility to infection via disruption of phagocyte functions. Nat Immunol. 2016;17(12):1361–72.

17. Palmer K, Coggon D. Does occupational exposure to iron promote infection? Occup Environ Med. 1997;54(8):529–34.

18. Nuorti JP, Butler JC, Farley MM, Harrison LH, McGeer A, Kolczak MS, et al. Cigarette smoking and invasive pneumococcal disease. N Engl J Med. 2000;342(10):681–9.

19. Cordes LG, Brink EW, Checko PJ, Lentnek A, Lyons RW, Hayes PS, et al. A cluster of Acinetobacter pneumonia in foundry workers. Ann Int Med. 1981;95(6):688–93.

20. Boelaert JR, Vandecasteele SJ, Appelberg R, Gordeuk VR. The Effect of the host's iron status on Tuberculosis. J Infect Dis. 2007;195(12):1745–53.

21.   Kao J-K, Wang S-C, Ho L-W, Huang S-W, Chang S-H, Yang R-C, et al. Chronic iron overload results in impaired bacterial killing of THP-1 derived macrophage through the inhibition of lysosomal acidification. PLoS ONE. 2016;11(5):e0156713.

22.   Philippot Q, Deslée G, Adair-Kirk TL, Woods JC, Byers D, Conradi S, et al. Increased iron sequestration in alveolar macrophages in chronic obstructive pulmonary disease. PLoS ONE. 2014;9(5):e96285.

23.   Verrills NM, Irwin JA, Yan He X, Wood LG, Powell H, Simpson JL, et al. Identification of novel diagnostic biomarkers for asthma and chronic obstructive pulmonary disease. Am J Respir Crit Care Med. 2011;183(12):1633–43.

24.   DeMeo DL, Mariani T, Bhattacharya S, Srisuma S, Lange C, Litonjua A, et al. Integration of genomic and genetic approaches implicates IREB2 as a COPD susceptibility gene. Am J Hum Genet. 2009;85(4):493–502.

25.   Cloonan SM, Glass K, Laucho-Contreras ME, Bhashyam AR, Cervo M, Pabón MA, et al. Mitochondrial iron chelation ameliorates cigarette smoke-induced bronchitis and emphysema in mice. Nat Med. 2016;22(2):163–74.

26.   Berenson CS, Kruzel RL, Eberhardt E, Dolnick R, Minderman H, Wallace PK, et al. Impaired innate immune alveolar macrophage response and the predilection for COPD exacerbations. Thorax. 2014;69(9):811–8.

27.   Morales-Nebreda L, Misharin AV, Perlman H, Budinger GRS. The heterogeneity of lung macrophages in the susceptibility to disease. Eur Respir Rev. 2015;24(137):505–9.

28.   Olakanmi O, McGowan SE, Hayek MB, Britigan BE. Iron sequestration by macrophages decreases the potential for extracellular hydroxyl radical formation. J Clin Invest. 1993;91(3):889–99.

29.   Corhay JL, Weber G, Bury T, Mariz S, Roelandts I, Radermecker MF. Iron content in human alveolar macrophages. Eur Respir J. 1992;5(7):804–9.

30.   Leigh R, Sharon RF, Efthimiadis AE, Hargreave FE, Kitching AD. Diagnosis of left-ventricular dysfunction from induced sputum examination. Lancet. 1999;354(9181):833–4.

31.   Winter WE, Bazydlo LAL, Harris NS. The Molecular biology of human iron metabolism. Lab Med. 2014;45(2):92–102.

32.   Wesselius L, Nelson M, Skikne B. Increased release of ferritin and iron by iron-loaded alveolar macrophages in cigarette smokers. Am J Respir Crit Care Med. 1994;150(3):690–5.

33.   Weinberg ED. Iron loading and disease surveillance. Emerging Infect Dis. 1999;5(3):346–52.

34.   Gan WQ, Man SFP, Senthilselvan A, Sin DD. Association between chronic obstructive pulmonary disease and systemic inflammation: a systematic review and a meta-analysis. Thorax. 2004;59(7):574–80.

35.   Nguyen NB. Hepcidin expression and iron transport in alveolar macrophages. Am J Physiol Lung Cell Mol Physiol. 2006;291(3):L417–25.

36.   Mohan S, Ho T, Kjarsgaard M, Radford K, Borhan ASM, Thabane L, et al. Hemosiderin in sputum macrophages may predict infective exacerbations of chronic obstructive pulmonary disease: a retrospective observational study. BMC Pulm Med. 2017;17(1):60.

37.   Finberg KE. Ironing out the role of Toll-like receptors. Blood. 2015;125(14):2183–4.

38.   Reid DW, Lam QT, Schneider H, Walters EH. Airway iron and iron-regulatory cytokines in cystic fibrosis. Eur Respir J. 2004;24(2):286–91.

39.   Meynard D, Sun CC, Wu Q, Chen W, Chen S, Nelson CN, et al. Inflammation Regulates TMPRSS6 Expression via STAT5. PLoS ONE. 2013;8(12):e82127–10.

40.   Sow FB, Nandakumar S, Velu V, Kellar KL, Schlesinger LS, Amara RR, et al. Mycobacterium tuberculosis components stimulate production of the antimicrobial peptide hepcidin. Tuberculosis (Edinb). 2011;91(4):314–21.

41.   Michels K, Nemeth E, Ganz T, Mehrad B. Hepcidin and host defense against infectious diseases. PLoS Pathog. 2015;11(8):e1004998–14.

42.   Wang C-Y, Meynard D, Lin HY. The role of TMPRSS6/matriptase-2 in iron regulation and anemia. Front Pharmacol. 2014;5:114.

43.   Chambers JC, Zhang W, Li Y, Sehmi J, Wass MN, Zabaneh D, et al. Genome-wide association study identifies variants in TMPRSS6 associated with hemoglobin levels. Nat Genet. 2009;41(11):1170–2.

44. Sow FB, Florence WC, Satoskar AR, Schlesinger LS, Zwilling BS, Lafuse WP. Expression and localization of hepcidin in macrophages: a role in host defense against tuberculosis. J Leukoc Biol. 2007;82(4):934–45.

44. Harrington-Kandt R, Stylianou E, Eddowes LA, Lim PJ, Stockdale L, 45 N, et al. Hepcidin deficiency and iron deficiency do not alter tuberculosis susceptibility in a murine M.tb infection model. PLoS ONE. 2018;13(1):e0191038–17.

46. Abreu R, Quinn F, Giri PK. Role of the hepcidin-ferroportin axis in pathogen-mediated intracellular iron sequestration in human phagocytic cells. Blood Adv. 2018;2(10):1089–100.

47. Lim D, Kim KS, Jeong J-H, Marques O, kim H-J, Song M, et al. The hepcidin-ferroportin axis controls the iron content of Salmonella-containing vacuoles in macrophages. Nat Commun. 2018;9:1–12.

48. Frazier MD, Mamo LB, Ghio AJ, Turi JL. Hepcidin expression in human airway epithelial cells is regulated by interferon-γ. Respir Res. 2011;12(1):100.

49. Deschemin J-C, Mathieu JRR, Zumerle S, Peyssonnaux C, Vaulont S. Pulmonary iron homeostasis in hepcidin knockout mice. Front Physiol. 2017;8:359–14.

50. Kesimer M, Ford AA, Ceppe A, Radicioni G, Cao R, Davis CW, et al. Airway mucin concentration as a marker of chronic bronchitis. N Engl J Med. 2017;377(10):911–22.

51. Conrad ME, Umbreit JN. Pathways of iron absorption. Blood Cells Mol Dis. 2002;29(3):336–55.

52. Aali M, Caldwell A, House K, Zhou J, Chappe V, Lehmann C. Iron chelation as novel treatment for lung inflammation in cystic fibrosis. Med Hypotheses. 2017;104:86–8.

53. Yatmark P, Morales NP, Chaisri U, Wichaiyo S, Hemstapat W, Srichairatanakool S, et al. Effects of iron chelators on pulmonary iron overload and oxidative stress in β-thalassemic mice. Pharmacology. 2015;96(3-4):192–9.

54. Walker EM, Walker SM. Effects of iron overload on the immune system. Ann Clin Lab Sci. 2000;30(4):354–65.

55.   Wiener E. Impaired phagocyte antibacterial effector functions in β-thalassemia: a likely factor in the increased susceptibility to bacterial infections. Hematology. 2013;8(1):35–40.

56.   Paradkar PN, De Domenico I, Durchfort N, Zohn I, Kaplan J, Ward DM. Iron depletion limits intracellular bacterial growth in macrophages. Blood. 2008;112(3):866–74.

57.   Muñoz M, Gómez-Ramírez S, Bhandari S. The safety of available treatment options for iron-deficiency anemia. Expert Opin Drug Saf. 2018;17(2):149–59.

58.   Litton E, Xiao J, Ho KM. Safety and efficacy of intravenous iron therapy in reducing requirement for allogeneic blood transfusion: systematic review and meta-analysis of randomised clinical trials. BMJ. 2013;347:f4822–2.

59.   Berenson CS, Garlipp MA, Grove LJ, Maloney J, Sethi S. Impaired phagocytosis of nontypeable Haemophilus influenzae by human alveolar macrophages in chronic obstructive pulmonary disease. The Journal of Infectious Diseases. 2006 Nov 15;194(10):1375–84.

60.   Berenson CS, Kruzel RL, Eberhardt E, Sethi S. Phagocytic dysfunction of human alveolar macrophages and severity of chronic obstructive pulmonary disease. J Infect Dis 2013;208(12):2036–45.

61.   Taylor AE, Finney-Hayward TK, Quint JK, Thomas CMR, Tudhope SJ, Wedzicha JA, et al. Defective macrophage phagocytosis of bacteria in COPD. Eur Respir J. 2010;35(5):1039–47.

62.   Sethi S, Wrona C, Eschberger K, Lobbins P, Cai X, Murphy TF. Inflammatory profile of new bacterial strain exacerbations of chronic obstructive pulmonary disease. Am J Respir Crit Care Med. 2008;177(5):491–7.

63.   Sethi S, Maloney J, Grove L, Wrona C, Berenson CS. Airway inflammation and bronchial bacterial colonization in chronic obstructive pulmonary disease. Am J Respir Crit Care Med. 2006;173(9):991–8.

64.   Huang YJ, Boushey HA. The Sputum microbiome in chronic obstructive pulmonary disease exacerbations. Annals ATS. 2015;12 Suppl 2:S176–80.

65.   Boixeda R, Almagro P, Diez-Manglano J, Cabrera FJ, Recio J, Martin-Garrido I, et al. Bacterial flora in the sputum and comorbidity in patients with acute exacerbations of COPD. COPD. 2015;10:2581–91.

66.   King PT, Sharma R. The Lung immune response to nontypeable haemophilus influenzae (lung immunity to NTHi). J Immunol Res. 2015;3:1–14.

67.   Hurst JR, Vestbo J, Anzueto A, Locantore N, Müllerova H, Tal-Singer R, et al. Susceptibility to exacerbation in chronic obstructive pulmonary disease. N Engl J Med. 2010;363(12):1128–38.

68.   Woodruff PG, Agustí AG, Roche N, Singh D, Martinez FJ. Current concepts in targeting chronic obstructive pulmonary disease pharmacotherapy: making progress towards personalised management. Lancet. 2015;385(9979):1789–98.

69.   Agustí AG, Calverley PMA, Celli BR, Coxson HO, Edwards LD, Lomas DA, et al. Characterisation of COPD heterogeneity in the ECLIPSE cohort. Respir Res. 2010;11:122.

70.   Ho T, Dasgupta A, Hargreave FE, Nair P. The use of cellular and molecular biomarkers to manage COPD exacerbations. Exp Rev Respir Med. 2017;11(5):403–11.

71.   Gray RD, Duncan A, Noble D, Imrie M, O'Reilly DSJ, Innes JA, et al. Sputum trace metals are biomarkers of inflammatory and suppurative lung disease. Chest. 2010;137(3):635–41.

72.   Grebski E, Hess T, Hold G, Speich R, Russi E. Diagnostic value of hemosiderin-containing macrophages in bronchoalveolar lavage. Chest. 1992;102(6):1794–9.

73.   Gifford AH, Moulton LA, Dorman DB, Olbina G, Westerman M, Parker HW, et al. Iron homeostasis during cystic fibrosis pulmonary exacerbation. clinical and translational science. 2012;5(4):368–73.

74.   Pizzichini E, Pizzichini MMM, Efthimiadis AE, Evans S, Morris MM, Squillace D, et al. Indices of airway inflammation in induced sputum: reproducibility and validity of cell and fluid-phase measurements. Am J Respir Crit Care Med. 1996;154:308–17.